Quantum theory of nondegenerate four-wave mixing

M. D. Reid and D. F. Walls
Physics Department, University of Waikato, Hamilton, New Zealand
(Received 21 May 1986)

A fully quantum-mechanical theory of nondegenerate four-wave mixing in a system of two-level atoms is presented. The squeezing in the output field from an intracavity four-wave-mixing experiment is calculated. The theory is compared with the recent experimental results of Slusher, Hollberg, Yurke, Mertz, and Valley and strategies to improve the squeezing are suggested.

I. INTRODUCTION

Squeezed states of light represent a research field in quantum optics which is truly concerned with quantum features of the electromagnetic field. Squeezed states have fluctuations in one of the quadrature phases less than that of a coherent state.[1,2] They have potential applications in precision measurements[3] and communication systems.[4] For a review the reader is referred to Ref. 5.

Interest has accelerated recently due to the significant experimental effort being made to generate squeezed states of light[6-15] and particularly with the recent experimental observation[12] of light squeezed below the quantum (or coherent-state) limit. Several experimental groups are attempting to produce squeezed light and are using a variety of systems. The first experimental interest was shown by Shapiro *et al.*[6] who used four-wave mixing in sodium to try to squeeze the light field, and by Levenson and coworkers[7-10] who use four-wave mixing in an optical fiber. Both of these groups have succeeded in "squeezing" classical noise.[6,10] Four-wave mixing involves coupling of two pump photons with two weak-field photons via a nonlinear medium. The most successful experiment to date has been that of Slusher *et al.*,[11-14] who have reported what may be the first experimental observation of squeezed light. They employ intracavity four-wave mixing using a sodium atomic beam as the nonlinear medium. More recently, Kimble *et al.*[15] have been attempting to generate squeezed light using intracavity second-harmonic generation.

A number of optical systems have been predicted theoretically to produce squeezed states of light. These range from parametric amplification,[2,16-20] four-wave mixing,[21-25] dispersive optical bistability,[26,27] two-photon bistability,[28-30] and second-harmonic generation.[26,31] Small amounts of squeezing are possible in resonance fluorescence[32,33] and absorptive bistability.[27,28,34] There has been much interest recently also in generation of squeezed light in a Rydberg maser.[35-37] In this paper we shall develop the theory of four-wave mixing.

Four-wave mixing was first proposed by Yuen and Shapiro[21] as a means of generating squeezed light. They originally considered the backward configuration where the two weak-field waves (and the two pump waves) are counterpropagating. This is the configuration used in phase-conjugation experiments. More recently, Yurke[25] has suggested producing squeezed states using four-wave mixing in a single-port optical cavity. The cavity configuration has the advantage of increasing the interaction time between the nonlinear medium and field. Yurke calculated the squeezing in the experimentally accessible field external to the cavity. Both the models of Yurke and Yuen and Shapiro assume a phenomenological nonlinearity χ for the medium and found excellent squeezing to be attainable for sufficient nonlinearity so as to approach the threshold for oscillations.

However, modeling the medium by a classical susceptibility will not describe the quantum noise processes inherent in a real medium, such as the optical fiber in the experiments of Levenson *et al.*[8] or the atomic medium in the experiments of Bondurant *et al.*[6] and Slusher *et al.*[12] A medium will absorb radiation and the effect of the absorption on the squeezing were originally studied by Kumar and Shapiro[2] in a phenomenological manner. They suggested use of forward four-wave mixing in which the pump and weak fields are copropagating, as opposed to the counterpropagating situation. The experiment of Levenson, for example, is totally copropagating since the pump and weak fields propagate down the fiber in the same direction.

The models of Yuen and Shapiro,[21] Kumar and Shapiro,[22] and Yurke,[25] are phenomenological and could not describe correctly the effect of quantum fluctuations from the medium. For example, in the experiment of Slusher *et al.* the pump laser is closely tuned to the D_2 resonance of sodium. Hence one may model the medium in this situation as a two-level atom. The two-level atomic medium provides the nonlinear four-wave mixing which squeezes the light. However, in such a medium there is additional phase-insensitive fluorescent radiation present which tends to destroy the squeezing. Thus, fluorescence or spontaneous emission will impose a fundamental limitation on the squeezing possible in an experiment. A discussion of an experimental limit imposed by spontaneous emission is given by Slusher *et al.*[11]

The first fully quantum-mechanical treatment including the effect of spontaneous emission on squeezing for two-level atoms in a cavity was given for two-photon absorptive bistability and a two-photon laser by Lugiato and Strini[28] and Reid and Walls,[29] and for one-photon absorp-

 ©1986 The American Physical Society

tive bistability by Lugiato and Strini.[28] The effect of spontaneous emission in the lasing medium was to destroy the squeezing. Only a very small squeezing was predicted for the lower branch in one-photon absorptive bistability, a greater amount of squeezing being possible in the two-photon absorptive bistability. One may expect the effect of spontaneous emission to be less significant in dispersive bistability and four-wave mixing, systems which have also been better studied experimentally. We note also that the calculations[28,29] discussed above pertain to the squeezing in the internal-cavity mode rather than the squeezing in the output field which is experimentally accessible.

What may be the first calculation of the effect of quantum noise from a two-level atomic medium in a four-wave-mixing experiment was presented by Reid and Walls[23,24] for degenerate four-wave mixing. The term degenerate refers to both pump and weak fields at the same frequency. The totally forward degenerate situation in a ring cavity driven by an external laser field corresponds to the situation of dispersive optical bistability using two-level atoms and was also studied by Reid and Walls.[27] The calculations of Reid and Walls were based on techniques developed by Haken[38] for laser theory and Drummond and Walls[39] to describe quantum fluctuations in optical bistability.

The effect on the squeezing of fluorescence radiated from the two-level atoms for degenerate four-wave mixing was shown by Reid and Walls[24,27] to be significant. To obtain good squeezing, the intensity of the output light must be due primarily to the phase-sensitive four-wave-mixing coupling term and not to phase-insensitive fluorescence. Thus one needs intensities sufficient to enhance the nonlinearity (relative to both cavity loss and atomic loss) and yet low enough that one is still in a regime of very low atomic saturation. The latter is necessary to avoid fluorescence. The best squeezing is therefore predicted for a window of pump intensities. The implication is that high-atomic detuning and hence high intensities and cooperativity values are required for significant squeezing. Also the squeezing is sensitive to changes in parameters such as the cavity detuning (pump laser frequency[27]).

Thus one concludes from the analysis of the degenerate situation that the best strategy is to modify the experiment so as to minimize effects of spontaneous emission. Several suggestions have been made. A nonsaturating medium such as modeled by an anharmonic oscillator[40] will not give rise to the problems of two-level atomic fluorescence. The glass fiber used in Levenson's experiment was thought to be good from this point of view, but other noise sources have appeared.[9] Another possibility is to employ a different nonlinear mechanism such as is possible using two-photon transitions in three-level atoms.[30,41,42]

Another possibility and the one of interest to us here is to use the one-photon, two-level atomic transition as discussed above, but employing a nondegenerate four-wave-mixing scheme as opposed to a degenerate scheme. By nondegenerate we mean each of the two weak-intensity modes to be equally and oppositely detuned in frequency from the central pump mode. This is indeed the situation in the experiments of Shapiro and Slusher. The question of the effect of spontaneous emission in nondegenerate four-wave mixing was first raised by Slusher *et al.*[11] and our work has been largely motivated by comments made in that paper.

We indicate intuitively why the nondegenerate four-wave-mixing scheme may help in reducing fluorescence and produce better squeezing. Consider the fluorescence spectrum of a two-level atom pumped by a detuned intense laser field. The spectrum has an elastic peak at the pump frequency and at low intensities two inelastic peaks symmetrically displaced from the pump frequency by an amount corresponding to the atomic detuning. At higher intensities approaching saturation, the inelastic part of the spectrum becomes three peaked: two sidepeaks at the generalized Rabi frequencies and a central inelastic peak at the pump frequency. The center peak becomes proportionately larger at increasing intensities. It scatters phase-insensitive radiation back at the pump frequency and is thus the reason for sensitivity to fluorescence in degenerate four-wave mixing, where the squeezing is looked for in weak fields at that same pump frequency. The width of the fluorescent peak is of the order of the atomic linewidth $\gamma_\perp$. Intuitively, one would expect to be able to detune the weak fields from the central pump frequency over several atomic linewidths to avoid this fluorescence, and hence obtain better squeezing at higher pump intensities where fluorescence is a problem.

But in such nondegenerate four-wave mixing one is considering a four-wave-mixing coupling between weak fields detuned from the pump frequency, and thus from the frequency of the two-level atomic polarization. Does the coupling spectrum fade out also as one introduces a weak field detuning from the pump? The important criterion is the level of fluorescence compared to the nonlinear coupling. Thus to investigate whether nondegenerate four-wave mixing is advantageous to squeezing, one needs to compare both the fluorescence and the coupling spectra.

Nondegenerate four-wave mixing in two-level atomic media has been studied classically by Fu and Sargent[43] and Boyd *et al.*[44] The semiclassical loss-gain and coupling coefficient spectra have been derived. However, to describe squeezing a quantum theory is required.

A quantum theory applicable to nondegenerate four-wave mixing adapting the techniques of Scully and Lamb[45] has been presented by Sargent *et al.*[46–48] Reid and Walls[49–51] have also developed a quantum theory of nondegenerate four-wave mixing, adapting the techniques of Haken[38] and Drummond and Walls.[39] What may be the first results predicting advantages in squeezed-state generation via nondegenerate four-wave mixing have been presented by Reid and Walls,[49–51] who considered nondegenerate four-wave mixing in a high-Q optical cavity and calculated the squeezing in the field external to the cavity. They predicted significant advantages over the degenerate case in terms of avoiding phase insensitive fluorescence. Good squeezing was predicted possible for lower-atomic detunings and lower C values than the degenerate case, and for intensities saturating the atoms. There has been recent work also by Holm and Sargent[52] who extend the

calculations of Sargent *et al.*[47,48] to calculate the squeezing in the internal cavity field. They also predict enhancement of squeezing to be possible by detuning the weak fields from the pump field.

In this paper we present in detail a quantum theory of nondegenerate four-wave mixing, adapting the methods of Haken[38] and Drummond and Walls.[39] We consider nondegenerate mixing in an optical high-Q ring cavity containing a nonlinear medium which may be modeled as N two-level atoms. The cavity mode is pumped by an external laser. Four-wave mixing occurs between the pumped cavity mode and the two adjacent cavity modes. In a ring cavity these modes are all forward propagating. We assume a high-Q cavity such that the atomic variables may be adiabatically eliminated. The squeezing in the transmitted field external to the cavity and at the sideband frequencies is calculated, using techniques developed by Collett and Gardiner.[19,26,53] It is the squeezing in the field external to the cavity which is relevant experimentally, and this important point was first made by Yurke.[18]

We thus present in detail the derivation of equations and solutions previously published by Reid and Walls[49,51] and answer many of the questions raised in this introduction. We provide greater physical insight into previous results, as well as present new features. Wherever possible, we make comparisons with the semiclassical theory of Fu and Sargent[43] and Boyd *et al.*,[44] and the quantum theory of Sargent *et al.*[47] and Holm and Sargent.[52] We present a comparison of theoretical predictions with the experimental results of Slusher *et al.*[12]

We note that a good fit to the present experimental results has been provided by Klauder *et al.*[54] who use the degenerate theory of Reid and Walls[24] and includes effects such as phase jitter. Our results indicate that much better squeezing should in principle be attainable from nondegenerate four-wave mixing than has presently been observed.

II. DERIVATION OF QUANTUM-MECHANICAL EQUATIONS

We begin with a general description of nondegenerate four-wave mixing (Fig. 1) in an optical cavity. The medium is modeled as N two-level atoms, and is interacting with the radiation field at three frequencies. We write the model Hamiltonian in the electric-dipole and rotating-wave approximations as follows:

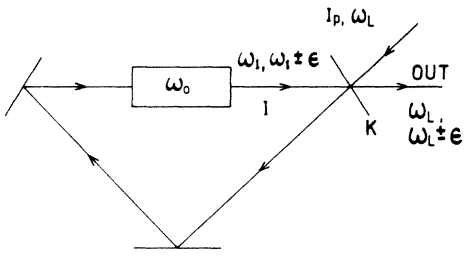

FIG. 1. Scheme for nondegenerate four-wave mixing in a ring cavity.

$$
\begin{aligned}
H &= \sum_{\mu=0}^{4} H_\mu \ , \\
H_0 &= \sum_{j=1}^{3} \hbar\omega_j a_j^\dagger a_j + \sum_{i=1}^{N} \hbar\omega_0 \sigma_{zi} \ , \\
H_1 &= i\hbar g \sum_{i=1}^{N} [\sigma_i (a_1^\dagger e^{-ik_1 r_i} + a_2^\dagger e^{-ik_2 r_i} + a_3^\dagger e^{-ik_3 r_i}) \\
&\qquad - \sigma_i^\dagger (a_1 e^{ik_1 r_i} + a_2 e^{ik_2 r_i} + a_3 e^{ik_3 r_i})] \ , \\
H_2 &= i\hbar (a_1^\dagger E e^{-i\omega_L t} - a_1 E^* e^{i\omega_L t}) \ , \\
H_3 &= \sum_{i=1}^{N} (\Gamma \sigma_i^\dagger + \Gamma^\dagger \sigma_i + \Gamma_p \sigma_{zi}) \ , \\
H_4 &= \sum_{j=1}^{3} \Gamma_c^\dagger a_j + \Gamma_c a_j^\dagger \ ,
\end{aligned}
\tag{1}
$$

a_1 is the boson annihilation operator of the pump mode at frequency ω_1. a_2 and a_3 are annihilation operators describing cavity modes at frequencies ω_2 and ω_3, such that $2\omega_1 = \omega_2 + \omega_3$ (and $2k_1 = k_2 + k_3$). We denote $\epsilon = \omega_1 - \omega_2$. $\sigma_i, \sigma_i^\dagger, \sigma_{zi}$ are spin operators describing the Nth two-level atom with atomic resonance frequency ω_0. The atomic reservoirs Γ and Γ_p describe energy loss from the atoms via spontaneous emission and phase damping or collisional processes, respectively. The loss of energy of the field cavity modes due to dissipation through the cavity mirrors is described by the field reservoir Γ_c. For simplicity we will assume the modes to be independently coupled to the external environment (Γ_c) and take the cavity decay rates to be equal to the same value, κ. We have allowed in our Hamiltonian for the situation where the pump mode a_1 is a resonant cavity mode driven by an external coherent input field E of frequency ω_1. In the case (Fig. 1) of a single cavity for both pump and sideband modes, we have assumed that the cavity detuning $\omega_1 - \omega_L$ is much smaller than the separation in frequency $\epsilon = \omega_1 - \omega_2$ between adjacent cavity modes, so that only mode a_1 is effectively pumped.

To study the Hamiltonian we adapt the treatment used by Drummond and Walls[39] to study the degenerate situation, where $\omega_j = \omega_1$ and $a_j = a$. The technique was first developed by Haken[38] for laser theory and extended for a quantum theory of optical bistability by Drummond and Walls.[39] To summarize, a master equation for the density operator ρ is derived using standard techniques.[55] A normally ordered characteristic function $\tilde{\chi}$ is defined (for the degenerate case)

$$
\tilde{\chi} = \mathrm{Tr} O \rho \tag{2}
$$

where

$$
O = e^{ie^\dagger S^\dagger} e^{i\eta S_z} e^{ieS} e^{i\beta^\dagger a^\dagger} e^{i\beta a}
$$

and

$$
S = \sum_{i=1}^{N} \sigma_i e^{-ik_1 r_i}, \quad S_z = \sum_{i=1}^{N} \sigma_{zi} \ .
$$

A distribution function f is the Fourier transform of the characteristic function

$$f=\int \chi e^{iv^{\dagger}e^{\dagger}}e^{iD\eta}e^{ive}e^{i\alpha^{\dagger}\beta^{\dagger}}e^{i\alpha\beta}d^2ed^2e^{\dagger}d^2\eta d^2\beta d^2\beta^{\dagger} \quad (3)$$

and one thus establishes a correspondence between c numbers and operators as follows:

$$\begin{aligned} &v\leftrightarrow S,\ v^{\dagger}\leftrightarrow S^{\dagger}\ ,\\ &D\leftrightarrow S_z\ ,\\ &\alpha\leftrightarrow a,\ \alpha^{\dagger}\leftrightarrow a^{\dagger}\ . \end{aligned} \quad (4)$$

The standard representation as used in laser theory[38] does not in general provide a Fokker-Planck equation with a positive definite diffusion matrix. Hence we use a generalized representation[39,56] of the type (3), where the resulting Fokker-Planck equation has a positive semidefinite diffusion matrix and one can apply Ito rules to write the equivalent stochastic differential (Langevin) equations. The daggered notation (e.g., $\alpha^{\dagger}$) was introduced by Drummond and Gardiner[56] for use with the generalized P representation in which pairs such as $(\alpha,\alpha^{\dagger})$ are not complex conjugate but independent complex variables.

The equation of motion for f is derived and contains infinite-order derivatives. With N (the total number of atoms interacting with the cavity mode) large one can use scaling arguments to ignore all but first- and second-order derivatives, and to imply that the order of the quantum noise terms (second-order derivatives) is small compared to the semiclassical (first-order derivative) terms. One can then transform the resulting Fokker-Planck equation into a stochastic differential equation (Ito calculus).

These final equations are (in the Schrödinger model), as derived by Drummond and Walls[39]

$$\begin{aligned} \dot{\alpha}&=Ee^{-i\omega_L t}-(\kappa+i\omega_1)\alpha+gv+\Gamma_{\alpha}\ ,\\ \dot{v}&=-(\gamma_{\perp}+i\omega_0)v+g\alpha D+\Gamma_v\ ,\\ \dot{D}&=-\gamma_{||}(D+N)-2g(v^{\dagger}\alpha+v\alpha^{\dagger})+\Gamma_D\ , \end{aligned} \quad (5)$$

and the corresponding "c.c." equation obtained by exchanging $\alpha\leftrightarrow\alpha^{\dagger}$, $v\leftrightarrow v^{\dagger}$, $\Gamma_v\leftrightarrow\Gamma_{v^{\dagger}}$, $\Gamma_{\alpha}\leftrightarrow\Gamma_{\alpha^{\dagger}}$, and complex coefficients with their complex conjugates. The terms Γ are Gaussian noise functions with zero mean, reflecting the quantum noise present and arise from the second-order derivatives or diffusion matrix of the Fokker-Planck equation. With these quantum noise terms Γ ignored, one obtains the usual semiclassical equations of motion. The nonzero correlations of the quantum noise terms are obtained from the Fokker-Planck diffusion matrix and are

$$\begin{aligned} \langle\Gamma_v(t)\Gamma_v(t')\rangle&=2g\alpha v\delta(t-t')\ ,\\ \langle\Gamma_{v^{\dagger}}(t)\Gamma_{v^{\dagger}}(t')\rangle&=2g\alpha^{\dagger}v^{\dagger}\delta(t-t')\ ,\\ \langle\Gamma_D(t)\Gamma_D(t')\rangle&=[2\gamma_{||}(D+N)\\ &\quad -4g(v^{\dagger}\alpha+v\alpha^{\dagger})]\delta(t-t')\ ,\\ \langle\Gamma_v(t)\Gamma_{v^{\dagger}}(t')\rangle&=(D+N)\gamma_p\delta(t-t')\ , \end{aligned} \quad (6)$$

$\gamma_{\perp}$ and $\gamma_{||}$ are the transverse and longitudinal relaxation rates of the two-level atom, respectively, while γ_p is the rate of collision-induced phase decay of the atoms ($\gamma_{\perp}=\gamma_p+\gamma_{||}/2$). These decay rates arise from the interaction [H_3 of Eq. (1)] of the atoms with reservoirs such as other modes of the radiation field (thus giving rise to $\gamma_{||}$ describing spontaneous emission) or other atoms (modeling collisions γ_p). We have assumed the thermal noise (detrimental to squeezing) from the field reservoir Γ_c to be zero, taking a low-temperature limit.

In the nondegenerate situation described by Hamiltonian (1), the polarization v oscillates at an infinite number of frequencies. The problem can be simplified somewhat if we recognize interest in the gain of the weak-field modes a_2 and a_3 in the presence of the strong central pump mode a_1. We are thus interested in a limit where the strong pump mode a_1 is treated correctly to all orders, describing the saturation of the medium, while the expressions for the weak fields a_2,a_3 are kept to first order only. Then the polarization will oscillate at three dominant frequencies ω_L, $\omega_L+\epsilon$, and $\omega_L-\epsilon$. Thus we expand the polarization and field into Fourier components and write

$$\begin{aligned} \alpha&=\alpha_1e^{-i\omega_L t}+\alpha_2e^{-i(\omega_L-\epsilon)t}+\alpha_3e^{-i(\omega_L+\epsilon)t}\ ,\\ v&=v_1e^{-i\omega_L t}+v_2e^{-i(\omega_L-\epsilon)t}+v_3e^{-i(\omega_L+\epsilon)t}\ . \end{aligned} \quad (7)$$

Examination of the equation describing the inversion D shows that D will oscillate at the frequencies $0,\pm\epsilon$. Hence we write

$$D=D_1+D_2e^{-i\epsilon t}+D_2^{\dagger}e^{i\epsilon t}\ . \quad (8)$$

Thus we establish the following correspondence between c numbers and operators:

$$\begin{aligned} &\alpha_j\leftrightarrow a_j,\ \alpha_j^{\dagger}\leftrightarrow a_j^{\dagger}\ ,\\ &v_1\leftrightarrow S_1=\sum_{i=1}^{N}e^{-ik_1r_i}\sigma_i,\ v_1^{\dagger}\leftrightarrow S_1^{\dagger}\ ,\\ &v_2\leftrightarrow S_2=\sum_{i=1}^{N}e^{-ik_2r_i}\sigma_i,\ v_2^{\dagger}\leftrightarrow S_2^{\dagger}\ ,\\ &v_3\leftrightarrow S_3=\sum_{i=1}^{N}e^{-ik_3r_i}\sigma_i,\ v_3^{\dagger}\leftrightarrow S_3^{\dagger}\ ,\\ &D_1\leftrightarrow S_z=\sum_{i=1}^{N}\sigma_{zi}\ ,\\ &D_2\leftrightarrow S_{z2}=\sum_{i=1}^{N}\sigma_{zi}e^{i(k_1-k_3)r_i},\ D_2^{\dagger}\leftrightarrow S_{z2}^{\dagger}\ . \end{aligned} \quad (9)$$

This is achieved by the characteristic function $\tilde{\chi}=\mathrm{Tr}\rho O$ where

$$O=O_AO_F \quad (10a)$$

and

$$\begin{aligned} O_A&=\exp\left[i\sum_{j=1}^{3}e_j^{\dagger}S_j^{\dagger}\right]\exp[i(\eta_1S_z+\eta_2S_{z2}+\eta_2^{\dagger}S_{z2}^{\dagger})]\\ &\quad\times\exp\left[i\sum_{j=1}^{3}e_jS_j\right]\\ &=\prod_{i=1}^{N}e^{ie_i^{\dagger}\sigma_i^{\dagger}}e^{i\eta_i\sigma_{zi}}e^{ie_i\sigma_i}\ ,\\ O_F&=\exp\left[i\sum_{j=1}^{3}\beta_j^{\dagger}a_j^{\dagger}\right]\exp\left[i\sum_{j=1}^{3}\beta_ja_j\right]\ , \end{aligned} \quad (10b)$$

and

$$
\begin{aligned}
e_i &= e_1 e^{-ik_1 r_i} + e_2 e^{-ik_2 r_i} + e_3 e^{-ik_3 r_i} , \\
e_i^\dagger &= e_1^\dagger e^{ik_1 r_i} + e_2^\dagger e^{ik_2 r_i} + e_3^\dagger e^{ik_3 r_i} , \\
\eta_i &= \eta_1 + \eta_2 e^{i(k_1 - k_3) r_i} + \eta_2^\dagger e^{-i(k_1 - k_3) r_i} .
\end{aligned} \tag{10c}
$$

The summations in j run over frequencies 1,2,3 while i runs over the atoms.

The c-number Langevin equations for the variables (9) are most easily derived by substituting (7) and (8) into the equations (5) and matching terms of the same frequency, retaining to first order only terms in α_2, α_3, v_2, v_3, D_2, etc.

Alternatively, one derives the equation of motion for the new distribution function f, the Fourier transform of the characteristic function (10), along the lines described for the degenerate situation, making use of the latter form (10b) and (10c) of the characteristic function. One then neglects terms (not frequency matched) involving summations of functions such as $e^{i\Delta k r_i}$ ($\Delta k \neq 0$) over all the atoms. These terms are small compared to those phase- (or frequency-) matched terms for which $\Delta k = 0 = 2k_1 - k_2 - k_3$. Again only terms linear in the weak fields are retained. We assume the weak fields α_2, α_3 have no feedback effect on the strong pump mode α_1.

The final nondegenerate c-number equations in the above approximations are [in the rotating frame defined by (7)]

$$
\begin{aligned}
\dot{\alpha}_1 &= E - \kappa(1+i\phi)\alpha_1 + g v_1 , \\
\dot{\alpha}_2 &= -\kappa(1+i\phi)\alpha_2 + g v_2 , \\
\dot{\alpha}_3 &= -\kappa(1+i\phi)\alpha_3 + g v_3 , \\
\dot{v}_1 &= -\gamma_1 v_1 + g\alpha_1 D_1 + \Gamma_{v1} , \\
\dot{v}_2 &= -\gamma_2 v_2 + g\alpha_2 D_1 + g\alpha_1 D_2^\dagger + \Gamma_{v2} , \\
\dot{v}_3 &= -\gamma_3 v_3 + g\alpha_1 D_2 + g\alpha_3 D_1 + \Gamma_{v3} , \\
\dot{D}_1 &= -\gamma_{\|}(D_1 + N) - 2g(\alpha_1 v_1^\dagger + \alpha_1^\dagger v_1) + \Gamma_{D1} , \\
\dot{D}_2 &= -\gamma D_2 - 2g(\alpha_1 v_2^\dagger + \alpha_2^\dagger v_1 + \alpha_1^\dagger v_3 + \alpha_3 v_1^\dagger) + \Gamma_{D2} ,
\end{aligned} \tag{11a}
$$

and c.c. equations. We define

$$
\begin{aligned}
&\phi = (\omega_1 - \omega_L)/\kappa , \quad \gamma_j = \gamma_\perp(1 + i\Delta_j) , \quad \gamma = \gamma_{\|}(1 - i\delta) , \\
&\Delta_1 = (\omega_0 - \omega_L)/\gamma_\perp , \quad \Delta_2 = \Delta_1 + 2\delta f , \quad \Delta_3 = \Delta_1 - 2\delta f , \\
&\delta = \epsilon/\gamma_{\|} , \\
&f = \gamma_{\|}/2\gamma_\perp ,
\end{aligned} \tag{11b}
$$

f is the collisional parameter ($f = 1$ corresponds to no collisions, $f = 0$ is total collisional broadening). A diagrammatic illustration of the definitions of the above parameters is provided in Fig. 2. The nonzero noise correlations are, taking dominant terms in the pump only,

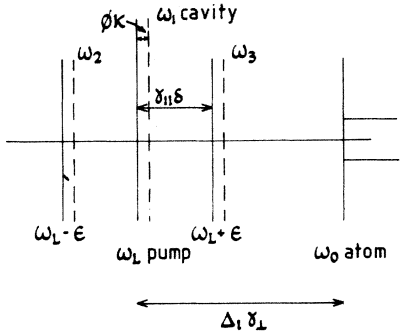

FIG. 2. Diagrammatic sketch of the parameters used in this paper.

$$
\begin{aligned}
\langle \Gamma_{v_2}(t)\Gamma_{v_3}(t')\rangle &= \langle \Gamma_{v_1}(t)\Gamma_{v_1}(t')\rangle \\
&= 2g\alpha_1 v_1 \delta(t - t') , \\
\langle \Gamma_{v_2^\dagger}(t)\Gamma_{v_3^\dagger}(t')\rangle &= \langle \Gamma_{v_1^\dagger}(t)\Gamma_{v_1^\dagger}(t')\rangle \\
&= 2g\alpha_1^\dagger v_1^\dagger \delta(t - t') , \\
\langle \Gamma_{D_2}(t)\Gamma_{D_2}(t')\rangle &= \langle \Gamma_{D_2^\dagger}(t)\Gamma_{D_2^\dagger}(t')\rangle \\
&= \langle \Gamma_{D_1}(t)\Gamma_{D_1}(t')\rangle \\
&= [2\gamma_{\|}(D_1 + N) - 4g(v_1^\dagger \alpha_1 + v_1 \alpha_1^\dagger)]\delta(t - t') .
\end{aligned} \tag{12}
$$

III. FIELD EQUATIONS IN THE HIGH-Q-CAVITY LIMIT

In the limit of a high-Q cavity such that $\kappa \ll \gamma_\perp, \gamma_{\|}$, one is justified in adiabatically eliminating the atomic variables. We set $\dot{v}_j = \dot{D}_1 = \dot{D}_2 = 0$ and solve for the atomic variables in terms of the field variables. The final equations in this limit are

$$
\dot{\alpha}_1 = E - \kappa(1+i\phi)\alpha_1 - \frac{2C\kappa\alpha_1}{(1+i\Delta_1)\Pi(0)} + F_{\alpha 1}(t) , \tag{13a}
$$

$$
\dot{\alpha}_2 = -\kappa\gamma(\delta)\alpha_2 + \kappa\chi(\delta)\alpha_3^\dagger e^{2i\theta_0} + F_{\alpha 2}(t) , \tag{13b}
$$

$$
\dot{\alpha}_3 = -\kappa\gamma(-\delta)\alpha_3 + \kappa\chi(-\delta)\alpha_2^\dagger e^{2i\theta_0} + F_{\alpha 3}(t) , \tag{13c}
$$

and the corresponding c.c. equations. We define $\gamma(\delta) = 1 + i\phi + \gamma_R(\delta) + i\gamma_I(\delta)$, $\chi(\delta) = \chi_R(\delta) + i\chi_I(\delta)$, and $\Pi(0) = 1 + I/1 + \Delta_1^2$. $F_i(t)$ are fluctuating noises with $\langle F_i(t)\rangle = 0$ and the nonzero noise correlations for the sidebands are

$$
\begin{aligned}
&\langle F_{\alpha 2}(t) F_{\alpha 3}(t)\rangle = \kappa R e^{2i\theta_0}\delta(t - t') , \quad R = R_R + iR_I , \\
&\langle F_{\alpha 2^\dagger}(t) F_{\alpha 3^\dagger}(t)\rangle = \kappa R^* e^{-2i\theta_0}\delta(t - t') , \\
&\langle F_{\alpha 2}(t) F_{\alpha 2^\dagger}(t')\rangle = \langle F_{\alpha 3}(t) F_{\alpha 3^\dagger}(t')\rangle \\
&\qquad = \kappa\Lambda\delta(t - t') .
\end{aligned} \tag{14}
$$

The coefficients γ_R, γ_I, χ, R, and Λ are functions of the following major scaled parameters [refer to Eq. (11b) for

definitions]: δ, the detuning of the sidemodes from the central pump mode in units of $\gamma_{||}$; Δ_1, the detuning of the central pump mode from the atomic resonance in units of $\gamma_\perp$; $C=g^2N/2\gamma_\perp\kappa$, the cooperativity parameter of the cavity; $I=|\alpha_1^{ss}|^2/n_0$ the steady-state intracavity pump intensity in units of n_0 the resonant saturation intensity, where $n_0=\gamma_{||}\gamma_\perp/4g^2$, $\alpha_1^{ss}=|\alpha_1^{ss}|e^{i\theta_0}$ is the steady-state semiclassical solution of the equation (13a) for the cavity pump mode, and f is the collisional parameter. The solutions are

$$\gamma_R(\delta)=\frac{2C\{1+I[a-c+\Delta_2(d-b)]+I^2[bd-ac+\Delta_2(ad+cb)]\}}{(1+\Delta_2^2)\Pi(0)|\Pi(\delta)|^2},$$

$$\gamma_I(\delta)=\frac{2C\{-\Delta_2+I[d-b-\Delta_2(a-c)]+I^2[ad+bc-\Delta_2(bd-ac)]\}}{(1+\Delta_2^2)\Pi(0)|\Pi(\delta)|^2},$$

$$\chi_R(\delta)=\frac{2CI\{e-\delta fq+I[ae+bq+\delta f(be-aq)]\}}{\Pi(0)|\Pi(\delta)|^2(1+\delta^2)(1+\Delta_1^2)(1+\Delta_2^2)(1+\Delta_3^2)},$$

$$\chi_I(\delta)=\frac{2CI\{q+\delta fe+I[aq-be+\delta f(ae+bq)]\}}{\Pi(0)|\Pi(\delta)|^2(1+\delta^2)(1+\Delta_1^2)(1+\Delta_2^2)(1+\Delta_2^3)},$$

$$\Lambda=\frac{2CI^2[1+\Delta_3^2+f-f\Delta_1\Delta_3+\delta(\Delta_1+\Delta_3)+If/2]}{\Pi(0)|\Pi(\delta)|^2(1+\delta^2)(1+\Delta_1^2)(1+\Delta_2^2)(1+\Delta_3^2)},$$

$$R_R=\frac{-2CI[f(1+\delta^2)r+IA(r,s)+I^2fB(r,s)]}{\Pi(0)|\Pi(\delta)|^2(1+\delta^2)(1+\Delta_1^2)(1+\Delta_2^2)(1+\Delta_3^2)},$$

$$R_I=\frac{-2CI\{-f(1+\delta^2)s+I[A(-s,r)+P_1]+I^2f[B(-s,r)+P_2]\}}{\Pi(0)|\Pi(\delta)|^2(1+\delta^2)(1+\Delta_1^2)(1+\Delta_2^2)(1+\Delta_3^2)},$$

$$P_1=\Delta_2+\Delta_3-\Delta_2\Delta_3+1,\quad P_2=(\Delta_1-1)/4$$

$$a=\frac{2+\Delta_3^2+\Delta_2^2-\delta\Delta_2(1+\Delta_3^2)+\delta\Delta_3(1+\Delta_2^2)}{2(1+\delta^2)(1+\Delta_2^2)(1+\Delta_3^2)},$$

$$b=\frac{-\delta(2+\Delta_3^2+\Delta_2^2)-\Delta_2(1+\Delta_3^2)+\Delta_3(1+\Delta_2^2)}{2(1+\delta^2)(1+\Delta_2^2)(1+\Delta_3^2)},$$

$$c=\frac{(\Delta_3-\Delta_1)(\Delta_3+\Delta_1-\delta+\delta\Delta_3\Delta_1)}{2(1+\delta^2)(1+\Delta_3^2)(1+\Delta_1^2)},$$

$$d=\frac{(\Delta_3-\Delta_1)[1-\Delta_3\Delta_1+\delta(\Delta_3+\Delta_1)]}{2(1+\delta^2)(1+\Delta_3^2)(1+\Delta_1^2)},$$

$$e=1+\Delta_3\Delta_1+\Delta_2\Delta_3-\Delta_2\Delta_1+\delta(\Delta_3-\Delta_1-\Delta_2-\Delta_2\Delta_3\Delta_1), \tag{15}$$

$$q=\Delta_3-\Delta_1-\Delta_2-\Delta_2\Delta_3\Delta_1-\delta(1+\Delta_3\Delta_1+\Delta_2\Delta_3-\Delta_2\Delta_1),$$

$$\Pi(\delta)=\Pi_R+i\Pi_I,\quad \Pi_R=1+aI,\quad \Pi_I=bI,$$

$$A(r,s)=f(1+\delta^2)2ar-f(rg+ms)/(1+\Delta_2^2)(1+\Delta_3^2)-1+\Delta_2\Delta_3,$$

$$B(r,s)=\tfrac{1}{4}+(1+\delta^2)(a^2+b^2)r-\frac{[rag+rbh+ams+bns-r(1-\Delta_2\Delta_3)/4+s(\Delta_2+\Delta_3)/4]}{(1+\Delta_2^2)(1+\Delta_3^2)},$$

$$r=1-\Delta_2\Delta_3-\Delta_1\Delta_2-\Delta_1\Delta_3,$$

$$s=\Delta_2+\Delta_3+\Delta_1-\Delta_1\Delta_2\Delta_3,$$

$$2g=(1+\Delta_3^2)(1-\Delta_2\delta)+(1+\Delta_3\delta)(1+\Delta_2^2),$$

$$2h=-(1+\Delta_3^2)(\Delta_2+\delta)+(1+\Delta_2^2)(\Delta_3-\delta),$$

$$2m=-(1+\Delta_3^2)(\Delta_2+\delta)-(1+\Delta_2^2)(\Delta_3-\delta),$$

$$2n=-(1+\Delta_3^2)(1-\Delta_2\delta)+(1+\Delta_2^2)(1+\Delta_3\delta).$$

The steady-state cavity pump intensity I satisfies

$$I_p = I\left[\left[1+\frac{2C}{(1+\Delta_1^2)\Pi(0)}\right]^2+\left[\phi-\frac{2C\Delta_1}{(1+\Delta_1^2)\Pi(0)}\right]^2\right], \tag{16}$$

where $I_p = 4g^2|E/\kappa|^2/\gamma_{\parallel}\gamma_{\perp}$ is the scaled external driving field. The phase θ_0 of the steady-state cavity pump is shifted from the phase of the external driving field E (which we take real for convenience) by

$$\tan\theta_0 = -\left[\phi-\frac{\Delta_1 2C}{(1+\Delta_1^2)\Pi(0)}\right]\Big/\left[1+\frac{2C}{(1+\Delta_1^2)\Pi(0)}\right].$$

One may expand to first order the pump field α_1 about a stable steady-state value α_1^{ss} ($\alpha_1=\alpha_1^{ss}+\delta\alpha$) and hence examine the statistics of the pump mode in the linear approximation used here. Indeed the squeezing in the field at frequency ω_l external to the cavity has been calculated by Reid and Walls,[27] the equation for $\delta\alpha$ being simply that for α_2 with $\delta=0$. The results of the paper[27] are thus reproduced in this work by selecting $\delta=0$.

Several comments relating to our basic equations (13) are relevant. The $F_{\alpha j}(t)$ are quantum noise terms necessary to preserve the commutation relation $[a,a^{\dagger}]=1$ and are not present in a semiclassical treatment. The equations for the classical field amplitudes are obtained by taking the expectation values $\langle\alpha_j\rangle$ in which case the noise terms $\langle F_{\alpha j}(t)\rangle$ vanish. These classical equations describing nondegenerate four-wave mixing in a two-level atomic medium have been derived previously by Fu and Sargent[43] and Boyd *et al.*[44] To calculate quantum features of the field, such as the squeezing, it is necessary to incorporate the quantum noise terms $F_{\alpha j}(t)$ and hence their correlations R and Λ.

The physical interpretation of the expressions $\gamma_R(\delta)$, $\gamma_I(\delta)$, $\chi(\delta)$, R, and Λ will be discussed in some detail. Firstly, $\gamma_R(\delta)$ is the loss-gain coefficient of the mode α_2, while $\gamma_I(\delta)$ is the dispersive response for mode α_2. $\chi(\delta)$ is the semiclassical coupling coefficient, giving rise to the generation of mode α_2 in the presence of the pump mode α_1 and weak field α_3. The expressions for the semiclassical coefficients $\gamma_R(\delta)$, $\gamma_I(\delta)$, and $\chi(\delta)$ are identical to those derived previously by Fu and Sargent and Boyd *et al.* To gain physical insight into the solutions, we revise results discussed in particular by Boyd *et al.*[44]

The behavior of a two-level atom with resonance frequency ω_0 when irradiated by a closely tuned laser at frequency ω_L has been well studied (Fig. 3). At low field intensities, inelastic scattering of laser photons occurs at the frequencies $2\omega_L-\omega_0$ and ω_0 (i.e., $\omega_L\pm\gamma_{\perp}\Delta_1$). This is brought about by the virtual process depicted in Fig. 3(a) involving the absorption of two laser photons and emission of photons at frequencies ω_0 and $2\omega_L-\omega_0$. The photons at frequency ω_0 undergo loss due to absorption while the photons at frequency $2\omega_L-\omega_0$ can show gain due to the scattering process described. This feature shows clearly in the plots of the absorption profile $\gamma_R(\delta)$ (Fig. 4) to be discussed below.

At higher intensities the atom saturates and Stark shifting of the atomic energy levels occurs. In the dressed atom each energy level splits into a pair separated in energy by the generalized Rabi frequency Ω [Fig. 3(b)]

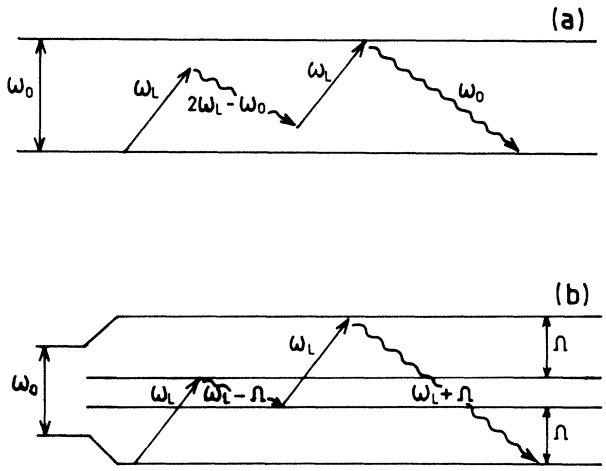

FIG. 3. Inelastic scattering of laser light of frequency ω_L by a two-level atom with resonance frequency ω_0: (a) at low intensities light is scattered at frequencies ω_L and $2\omega_L-\omega_0$; (b) at higher intensities saturating the atoms, light is scattered at the frequencies $\omega_L\pm\Omega$.

$$\Omega/\gamma_{\perp} = (2I+\Delta_1^2)^{1/2}. \tag{17}$$

The inelastic scattering process now involves two laser photons at frequency ω_L and scattered photons at frequencies $\omega_L-\Omega$ and $\omega_L+\Omega$ as depicted in Fig. 3(b).

The inelastic scattering process and Stark shift are evident in Fig. 4, showing plots of the quantity $\gamma_R(\delta)$ versus the detuning δ of the sideband from the pump, for various pump intensities I and detunings Δ_1 of the pump from the atomic resonance. Figure 4(a) illustrates the loss-gain profile on resonance ($\Delta_1=0$). As saturation occurs the initial single peak splits into a three-peaked spectrum. The frequencies of the three peaks correspond to those of resonance fluorescence: a central inelastic peak at the pump frequency, and two sidepeaks at the Rabi frequencies $|\delta|=\Omega/2\gamma_{\perp}$. These frequencies represent the three absorption frequencies possible in the dressed atom [Fig. 3(b)]. Figures 4(b) and 4(c) are for a detuned atom ($\Delta_1=4,100$). Particularly as saturation occurs, the profile shows peaks shifted from the pump frequency ω_L (corresponding to $\delta=0$) by the generalized Rabi frequency (17). The wave at $\delta=-\Omega/2\gamma_{\perp}$ (corresponding to frequency $\omega_L+\Omega$) is closest to the atomic resonance ω_0 and shows absorption. The mode at frequency $\omega_L-\Omega$ can show gain due to the inelastic scattering process depicted in Fig. 3 and being farther away from the atomic resonance ω_0. The gain at $\omega_L-\Omega$ is more significant as the pump intensity I increases above the saturation level. At higher intensities, regions of gain appear between the two peaks. The graph at $\Delta_1=100$ [Fig. 4(c)] contains sharper peaks as the generalized Rabi frequency (17) is increased. Saturation for large detunings corresponds to I of the order Δ_1^2.

Figure 5 shows the dispersive profile $\gamma_I(\delta)$. Below saturation, clear resonant behavior is seen at the frequency

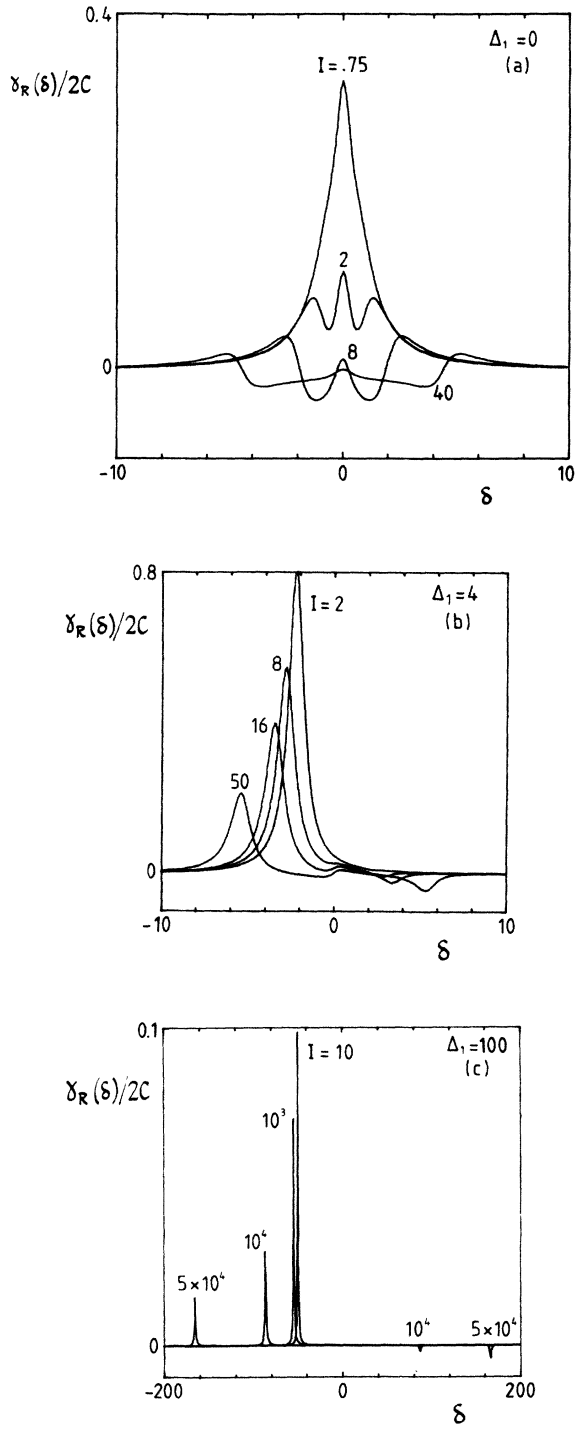

FIG. 4. Absorption profile $\gamma_R(\delta)$: (a) $\Delta_1=0$, (b) $\Delta_1=4$, (c) $\Delta_1=100$.

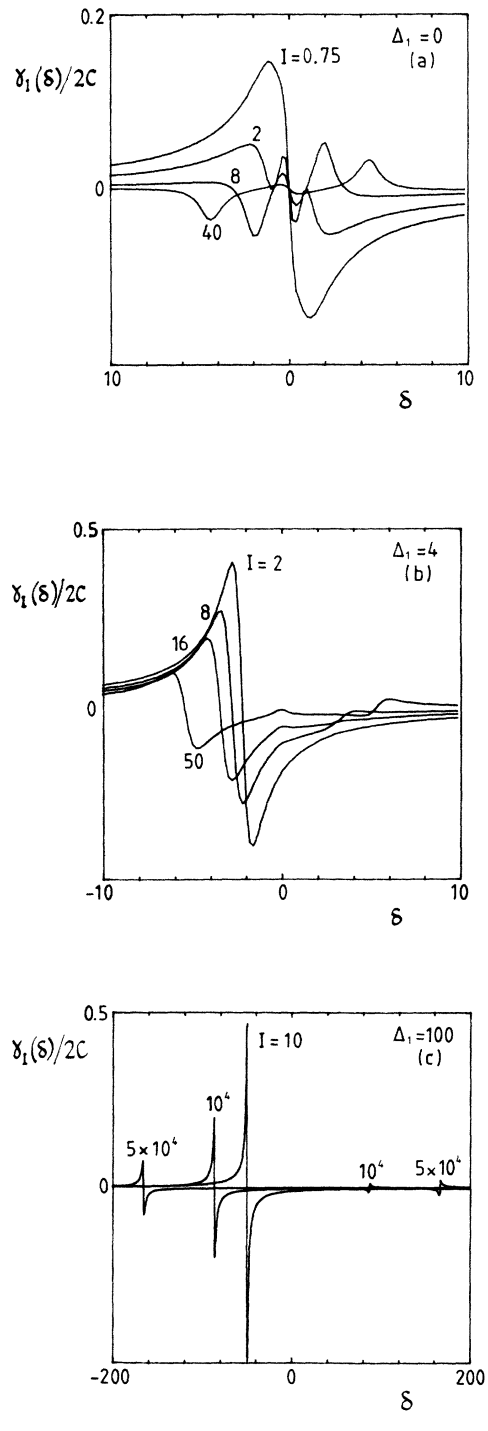

FIG. 5. Dispersion profile $\gamma_I(\delta)$: (a) $\Delta_1=0$, (b) $\Delta_1=4$, (c) $\Delta_1=100$.

$\omega_L+\Omega$ ($\delta=-\Omega/2\gamma_\perp$) closest to the atomic resonance ω_0. As saturation occurs smaller resonances are detectable at ω_L and $\omega_L-\Omega$.

The inelastic scattering process discussed above and depicted in Fig. 3 will be important in understanding some of the key effects discussed later in this paper and concerning calculations of squeezing. One has, in our four-wave mixing system, in addition to the pump laser at frequency ω_L, two weaker fields of frequencies $\omega_L\pm\epsilon$. The sidemodes are coupled via the four-wave parametric coupling specified by the $\chi(\delta)$ and R terms in Eqs. (13) and (14). Such a four-wave interaction is responsible for the significant squeezing possible in this system. The four-wave-mixing process is often symbolized in simple terms

by a phenomenological Hamiltonian as follows:

$$H = h\chi(a_1^\dagger)^2 a_2 a_3 + h\chi a_1^2 a_2^\dagger a_3^\dagger , \tag{18}$$

a_1 is the boson operator for the pump mode at frequency ω_L, and a_2 and a_3 are the sideband modes at frequencies $\omega_L - \epsilon$ and $\omega_L + \epsilon$, respectively. The Hamiltonian is the original prototype[2,5] predicted to give excellent squeezing in a suitable combination of modes a_2 and a_3. This is provided the pump a_1 is of sufficient intensity that it may be treated classically and nondepleting, and also that the nonlinear coupling χ is sufficiently large. In this simple model, the larger the coupling χ the better the squeezing. Now the Hamiltonian (18) symbolizes destruction of two pump photons a_1 and creation of two sideband photons a_2 and a_3. This is precisely the process depicted in Fig. 3. As discussed above, this inelastic multiphoton scattering process is responsible for sidepeaks at the generalized Rabi frequency in the fluorescent spectrum. What we would like to consider, in terms of the squeezing possible, is the "coupling spectrum," i.e., $\chi(\delta)$. We will expect, in view of Fig. 3, an enhancement of coupling (i.e., sidepeaks in the coupling spectrum) at the generalized Rabi frequencies. Thus when the frequency of the weak fields coincides with that of the sidebands of the fluorescent intensity spectrum ($\epsilon \simeq \Omega$), one may expect a resonant enhancement of four-wave-mixing gain and also of squeezing possible. The inelastic scattering described above in qualitative terms has been shown responsible for resonant enhancement effects in four-wave mixing in a two-level-atom medium by Boyd *et al.*[44]

The coupling response $|\chi(\delta)|$, which may be thought of as the spectrum for four-wave mixing between sidebands, is plotted in Fig. 6. On resonance with the atoms $\Delta_1 = 0$, maximum coupling occurs near $\delta = 0$ at lower intensities. We point out that $\delta = 0$ corresponds to degenerate four-wave mixing. The spectrum splits into three peaks as saturation occurs. With a detuned atom, below saturation the maximum coupling $|\chi(\delta)|$ is at the doublet $\omega_L \pm \Omega$ ($\omega_0, 2\omega_L - \omega_0$). At higher intensities a small central peak appears, the frequencies of the coupling peaks then correspond to those of the Stark triplet ω_L, $\omega_L \pm \Omega$. Important to note is the small height of the central peak compared to the sidepeaks and the relatively flat nonzero coupling spectrum $|\chi(\delta)|$ over the range of frequencies between the Rabi frequencies, i.e., for $|\delta| < \Omega/2\gamma_\perp$. This is particularly noticeable on the plot for $\Delta_1 = 100$, where the central peak is very small. This flat region at such high atomic detunings is essentially the imaginary component $\chi_I(\delta)$. χ_R and χ_I show comparable peak heights only at the Rabi frequencies. The significant enhancement of coupling $\chi(\delta)$ at the Rabi frequencies is due to the inelastic scattering effect discussed above and illustrated in Fig. 3, and is a key effect discussed in this paper.

Of particular interest to us in calculations of physical importance are quantities such as the mean number of photons in the cavity $\langle a_2^\dagger a_2 \rangle$ and $\langle a_3^\dagger a_3 \rangle$. Particularly relevant for squeezing calculations are fluctuations such as $\langle a_j^\dagger a_j \rangle - \langle a_j^\dagger \rangle \langle a_j \rangle$ and $\langle a_2 a_3 \rangle - \langle a_2 \rangle \langle a_3 \rangle$. It is in such calculations that the quantum terms Λ and R are needed and their physical significance made clear. To gain insight into the physical meaning of Λ and R and to assist in making a direct comparison with the work of Sargent *et al.*,[46–48,52] we write the Fokker-Planck equation (for the generalized P function) equivalent to the Langevin equation (13):

$$\frac{\partial P}{\partial t} = -\left[\frac{\partial}{\partial \alpha_2} \kappa[-\gamma(\delta)\alpha_2 + \chi(\delta)\alpha_3^\dagger] + \text{c.c.} + \frac{\partial}{\partial \alpha_3} \kappa[-\gamma(-\delta)\alpha_3 + \chi(-\delta)\alpha_2^\dagger] + \text{c.c.} \right.$$
$$\left. + \frac{\partial^2}{\partial \alpha_2^\dagger \partial \alpha_2} \kappa\Lambda + \frac{\partial^2}{\partial \alpha_3^\dagger \partial \alpha_3} \kappa\Lambda \frac{\partial^2}{\partial \alpha_2 \partial \alpha_3} \kappa R + \frac{\partial^2}{\partial \alpha_2^\dagger \partial \alpha_3^\dagger} \kappa R^* \right] P . \tag{19}$$

The equation of motion for

$$\langle a_2^\dagger a_2 \rangle = \int P(\alpha_2, \alpha_3, \alpha_2^\dagger, \alpha_3^\dagger) \alpha_2^\dagger \alpha_2 d^2\alpha_2 d^2\alpha_2^\dagger d^2\alpha_3 d^2\alpha_3^\dagger$$

is derived from (19) by integration by parts and using boundary conditions for the P function. The result is written is written below and may be compared with similar equations derived by Sargent *et al.*:[46–48]

$$\frac{d}{dt}\langle a_2^\dagger a_2 \rangle = -2\kappa[\gamma_R(\delta) + 1]\langle a_2^\dagger a_2 \rangle + \kappa\chi(\delta)\langle a_2^\dagger a_3^\dagger \rangle + \kappa\chi^*(\delta)\langle a_2 a_3 \rangle + \kappa\Lambda , \tag{20a}$$

$$\frac{d}{dt}\langle a_3^\dagger a_3 \rangle = -2\kappa[\gamma_R(-\delta) + 1]\langle a_3^\dagger a_3 \rangle + \kappa\chi(-\delta)\langle a_2^\dagger a_3^\dagger \rangle + \kappa\chi^*(-\delta)\langle a_2 a_3 \rangle + \kappa\Lambda , \tag{20b}$$

$$\frac{d}{dt}\langle a_2 a_3 \rangle = -\kappa[\gamma(\delta) + \gamma(-\delta)]\langle a_2 a_3 \rangle + \kappa\chi(\delta)\langle a_3^\dagger a_3 \rangle + \kappa\chi(-\delta)\langle a_2^\dagger a_2 \rangle + \kappa R . \tag{20c}$$

As in the discussion in Ref. 46, imagine that one can decouple the sideband interaction so that $\chi(\delta) = \chi(-\delta) = 0$ and the correlation $\langle F_{\alpha 2}(t) F_{\alpha 3}(t') \rangle$ is zero ($R = 0$), i.e., the amplitude α_3 is zero in the equation for α_2 and vice versa. The equation for the cavity intensity at the sideband δ is then

$$\frac{d}{dt}\langle a_2^\dagger a_2 \rangle = -2\kappa[\gamma_R(\delta) + 1]\langle a_2^\dagger a_2 \rangle + \kappa\Lambda \tag{21}$$

and is thus due solely to fluorescence, detectable at δ, from the pumped two-level atom. The steady-state solu-

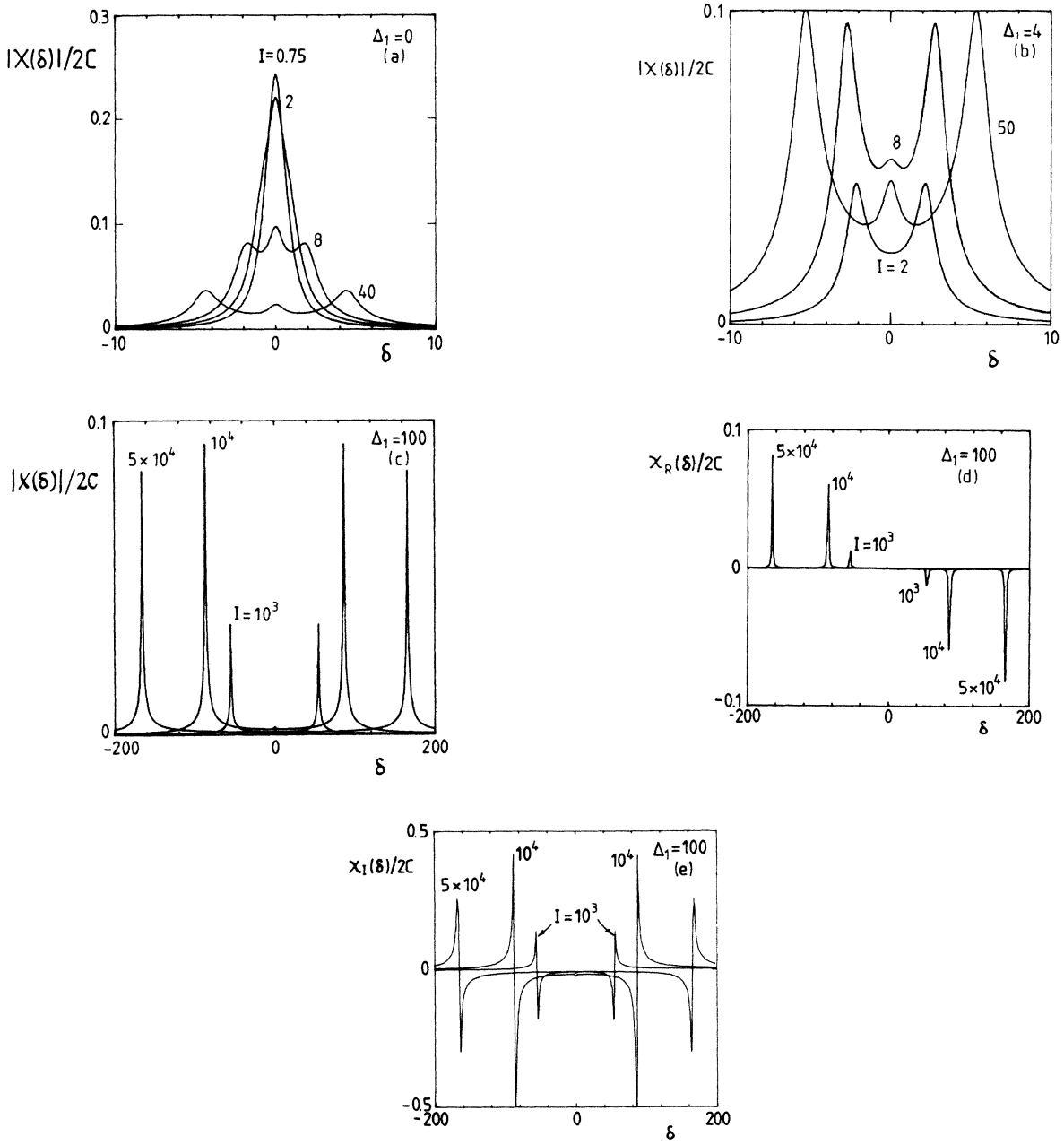

FIG. 6. Four-wave-mixing coupling response $|\chi(\delta)|$: (a) $\Delta_1=0$, (b) $\Delta_1=4$, (c) $\Delta_1=100$, (d) χ_R for $\Delta_1=100$, (e) χ_I for $\Delta_1=100$.

tion for the cavity intensity is then $\langle a_2^\dagger a_2\rangle = \Lambda/2\kappa[1+\gamma_R(\delta)]$. In the limit of a large cavity linewidth, or small cooperativity C, such that $\gamma_R(\delta)\ll 1$, the intensity due to this fluorescence is simply $\Lambda/2\kappa$. Λ itself may thus be thought of as the phase-insensitive fluorescence spectrum from the pumped two-level atom. We point out that as $\delta=0$, the solution to Eq. (20a) represents not the total intensity of the intracavity pump mode, but the first-order contribution in a linearized theory where the zeroth-order contribution is given by the deterministic steady-state solution (16). This additional zeroth-order coherent term at $\delta=0$ contributes a δ-function elastic part to the fluorescent intensity spectrum discussed above. It does not contribute to the fluctuations or squeezing of the field (since $\langle\alpha_i\alpha_j\rangle=\langle\alpha_i\rangle\langle\alpha_j\rangle$ for a coherent state).

Plots of the function Λ are shown in Fig. 7 for various detunings Δ_1 of the pump mode from the atom. Figure 7(a) is the absorptive case $\Delta_1=0$. At low intensities below saturation, the spectrum is single peaked. At very high pump intensity I, we have the usual resonance fluorescence curve, the sidepeaks corresponding to the Rabi frequencies $|\delta|\sim\Omega/2\gamma_\perp=\frac{1}{2}\sqrt{2I}$, and one third the height of the central (inelastic) peak. Figures 7(b) and 7(c) show

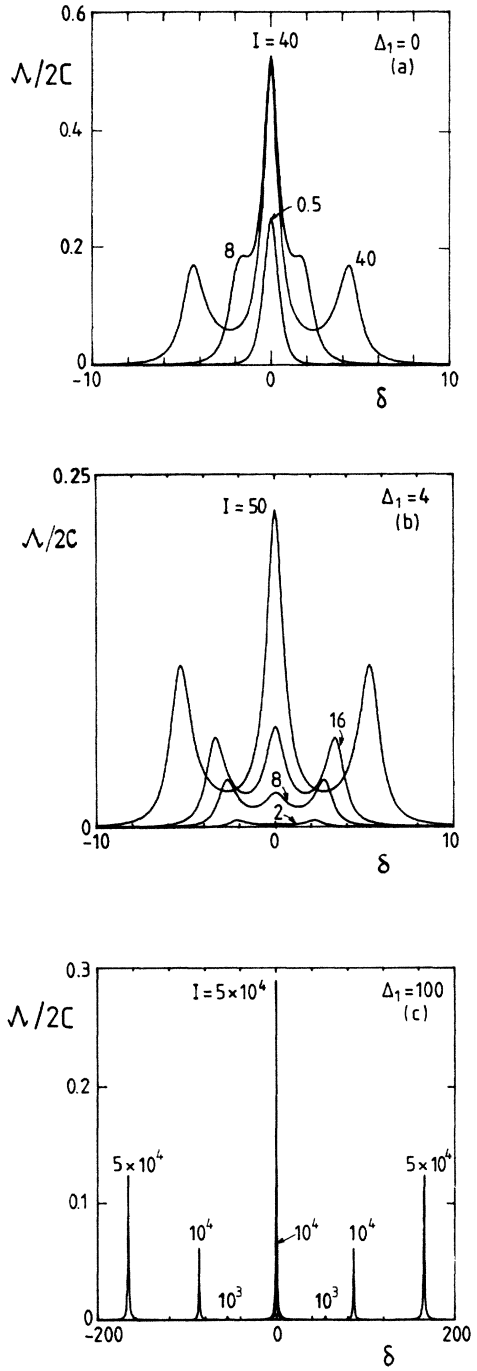

FIG. 7. Phase-insensitive fluorescence spectrum Λ: (a) $\Delta_1=0$, (b) $\Delta_1=4$, (c) $\Delta_1=100$.

the behavior for a detuned atom ($\Delta_1=4,100$). Below saturation, the spectrum is a doublet, with peaks at $|\delta|=\frac{1}{2}|\Delta_1|$. Again, in the high-intensity regime we have the usual fluorescence spectrum, showing three peaks at $\delta=0$ and $|\delta|=\Omega/2\gamma_\perp=\frac{1}{2}(2I+\Delta_1^2)^{1/2}$. The effect of the detuning Δ_1 is to reduce the heights of the three peaks, but to increase the relative height of the sidepeaks compared to the central peak. This effect is well known for fluorescence of a detuned two-level atom.

It is interesting to compare the fluorescence spectrum Λ for $\Delta_1=100$ [Fig. 7(c)] with the coupling spectrum $|\chi(\delta)|$ [Fig. 6(c)]. As the intensity increases towards the saturation intensity ($I=10^4$) the spectrum Λ develops a central peak, at $\delta=0$. The spectrum Λ shows three sharp peaks (width $\sim\gamma_\perp$) at $\delta=0$ and $\delta=\pm\Omega/2\gamma_\perp$, with low fluorescence between peaks. The spectrum for $|\chi(\delta)|$, on the other hand, is essentially a doublet (peaks at $\delta=\pm\Omega/2\gamma_\perp$), the central peak at $\delta=0$ being very small. This is to be expected, bearing in mind that $\chi(\delta)$ is the coefficient for coupling between a number of photons, as opposed to the fluorescence Λ which relates to emission of single photons. One would expect the coupling $\chi(\delta)$ to be enhanced at the Rabi frequencies $\delta=\pm\Omega/2\gamma_\perp$ corresponding to resonance with the process depicted in Fig. 3(b). The fluorescence Λ is enhanced at the frequencies $\delta=0$, $\pm\Omega/2\gamma_\perp$ corresponding to the transitions possible between the two pairs of energy levels of the dressed atom sketched in Fig. 3(b). We note also that the sidepeaks in the coupling spectrum are much broader than those of the fluorescence spectrum. The coupling spectrum for the region $|\delta|<\Omega/2\gamma_\perp$ is essentially flat and significant $[\chi(\delta)\sim\chi(0)\sim 2CI/\Delta_1^3]$ compared to the fluorescence Λ. This is of course with the exception of the very central $\delta=0$ region corresponding to the central fluorescent peak which dominates over the coupling $\chi(0)$ at higher intensities. The effect of the central peak of Λ has been shown by Reid and Walls[23,24,27] to detract from squeezing in degenerate ($\delta=0$) four-wave mixing. Thus regimes showing large four-wave-mixing coupling $\chi(\delta)$ with minimal fluorescence Λ are promising for production of squeezed light.

The second phase-sensitive noise term R is responsible for the squeezing effects we observe and is seen to be the driving term for $\langle a_2a_3\rangle$ in Eq. (20). For $R=0$, the steady-state solution for the phase-sensitive term $\langle a_2a_3\rangle$ is zero and hence there is no squeezing. In the dispersive (large detuning Δ_1) regime, R is closely related to $\chi(\delta)$, the four-wave-mixing coupling coefficient. Consider the following Hamiltonian, a perfect or "ideal squeezed state" producer:

$$H=\hbar\chi(a_2a_3+a_2^\dagger a_3^\dagger)\ . \tag{22}$$

The final c-number Langevin equations derived from this Hamiltonian are of the following form, in a generalized P representation:

$$\begin{aligned}\dot\alpha_2&=-i\chi\alpha_3^\dagger+F_{\alpha2}(t)\ ,\\ \dot\alpha_3&=-i\chi\alpha_2^\dagger+F_{\alpha3}(t)\ ,\end{aligned} \tag{23}$$

where the nonzero noise correlations are $\langle F_{\alpha2}(t)F_{\alpha3}(t')\rangle=-i\chi\delta(t-t')$. Thus a perfect squeezing situation for four-wave mixing corresponds in Eqs. (13) to $\Lambda=0$ and $R=\chi(\delta)=\chi(-\delta)$ and no loss γ. The "perfect" c-number equations (23) are equivalent to the operator equations

$$\begin{aligned}\dot a_2&=-i\chi a_3^\dagger\ ,\\ \dot a_3&=-i\chi a_2^\dagger\ ,\end{aligned} \tag{24}$$

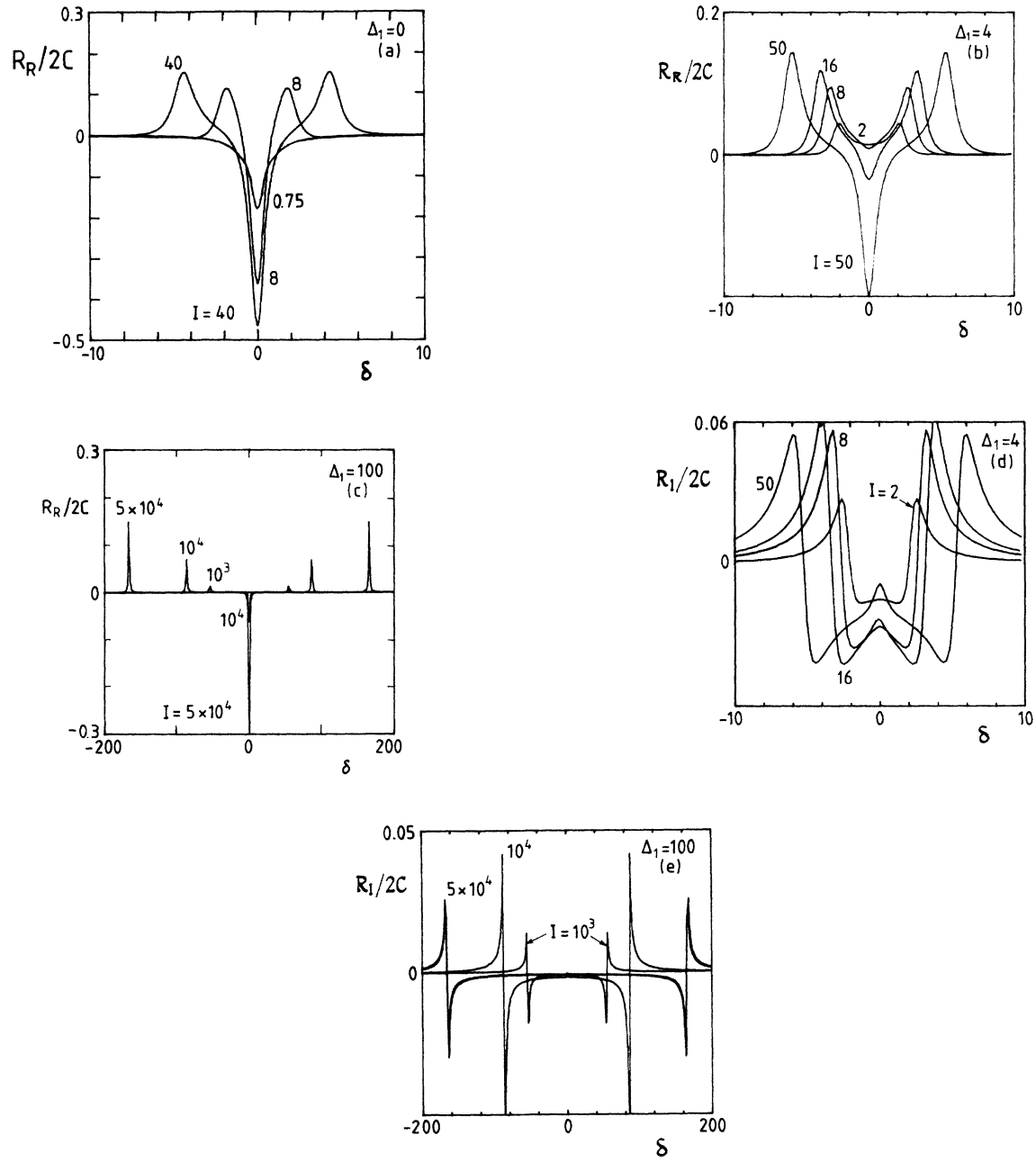

FIG. 8. Quantum coupling term $R=R_R+iR_I$: (a) R_R for $\Delta_1=0$, (b) R_R for $\Delta_1=4$, (c) R_R for $\Delta_1=100$, (d) R_I for $\Delta_1=4$, (e) R_I for $\Delta_1=100$. (Note $R_I=0$ at $\Delta_1=0$.)

which have been well studied for squeezing.[2,21]

The behavior of the phase-sensitive noise term R is summarized in Fig. 8. Plot 8(a) is for the atom pumped on resonance $\Delta_1=0$. Here R_I is zero, and R differs somewhat from the coupling $\chi(\delta)$. This graph should be compared with that of Λ for $\Delta_1=0$ (Fig. 7). R_R is similar to Λ but has a negative central peak and positive Rabi sidepeaks. Thus a graph of $\Lambda+R_R$ at $\Delta_1=0$ has a minimal central peak and Rabi sidebands of twice the height. This canceling of the central peak in the spectrum of $\Lambda+R_R$ was first pointed out by Sargent *et al.*,[46] who interpreted $\Lambda+R_R$ as the source term for the total number of photons at δ (for $\Delta_1=0$). R_R is thus a phase-sensitive fluorescence term relating to the amount of coupling between sidebands for the resonant situation $\Delta_1=0$. It describes the small amount of squeezing possible in absorptive optical bistability. As one increases the detuning Δ_1, the imaginary component R_I becomes nonzero. At $\Delta_1=100$, R_I is identical to $\chi_I(\delta)$ and dominates over $\chi_R(\delta)$, R_R, and Λ for regions away from the Rabi and central peaks. This is indicative of the good squeezing situation discussed with respect to the dispersive Hamiltoni-

an (22). R_I and $\chi_I(\delta)$, like the dispersive response $\gamma_I(\delta)$, have no significant central peak. This is unlike the real component R_R which remains similar to Λ (but with a negative peak) at all detunings Δ_1. Although R_I resembles $\chi_I(\delta)$ at higher detunings Δ_1, R_R is quite distinct from $\chi_R(\delta)$, which has no significant central peak at higher Δ_1, and Rabi peaks of opposite sign (Figs. 6 and 8). The behavior of the two-level atom precisely at the Rabi frequencies where fluorescence and absorption become resonant is not like that of the dispersive medium depicted by Hamiltonian (22). The R_R term is also resonant at the Rabi frequency and what squeezing is possible precisely at this frequency is to be studied in this paper.

A comparison can be made with the quantum nondegenerate mixing theory of Sargent *et al.*[46–48] and Holm and Sargent.[52] This theory represents an alternative approach to describe quantum-mechanically nondegenerate four-wave mixing and careful comparison with their work is thus very important. The above authors adapt the Scully-Lamb theory[45] developed for laser theory. The final master equation developed in their work is written [Eq. (100) of Ref. 47] in our notation for the boson operators:

$$\frac{\partial\rho}{\partial t}=-A_1(\rho a_2 a_2^\dagger-a_2^\dagger\rho a_2)-(B_1+\kappa)(a_2^\dagger a_2\rho-a_2\rho a_2^\dagger)$$
$$+D_1(\rho a_3^\dagger a_2^\dagger-a_2^\dagger\rho a_3^\dagger)+C_1(a_2^\dagger a_3^\dagger\rho-a_3^\dagger\rho a_2\dagger)$$
$$+(a_2\leftrightarrow a_3, A_1\rightarrow A_3,\ldots,D_1\rightarrow D_3)+\text{ adjoint}\ , \quad (25)$$

where the last term in parentheses is the same as the previous terms with the replacement of the appropriate variable. To make a direct comparison with our work, in particular with Eq. (19), a Fokker-Planck equation is developed from (25) in the generalized P distribution.[56] The method involves use of standard operator rules to convert operators into differential operators and use of boundary conditions for the P function so that one may integrate by parts. The method is standard and well explained in Refs. 55 and 56. The final Fokker-Planck equation corresponding to the work of Sargent *et al.* is

$$\frac{\partial P}{\partial t}=-\left\{\frac{\partial}{\partial\alpha_2}[(A_1-B_1-\kappa)\alpha_2+(C_1-D_1)\alpha_3^\dagger]+\text{c.c.}+\frac{\partial}{\partial\alpha_3}[(A_3-B_3-\kappa)\alpha_3+(C_3-D_3)\alpha_2^\dagger]+\text{c.c.}\right.$$
$$\left.+\frac{\partial^2}{\partial\alpha_2\partial\alpha_2}(A_1+A_1^*)+\frac{\partial^2}{\partial\alpha_3\partial\alpha_3}(A_3+A_3^*)+\frac{\partial^2}{\partial\alpha_2\partial\alpha_3}(C_1+C_3)+\frac{\partial^2}{\partial\alpha_2^\dagger\partial\alpha_3^\dagger}(C_1^*+C_3^*)\right\}P\ . \quad (26a)$$

This equation has the same form as the Fokker-Planck equation (19) derived from our results, provided one makes the following correspondence between our parameters and those of Sargent *et al.*:

$$\kappa[\gamma_R(\delta)+i\gamma_I(\delta)]=-A_1+B_1\ ,$$
$$\kappa[\gamma_R(-\delta)+i\gamma_I(-\delta)]=-A_3+B_3\ ,$$
$$\kappa\chi(\delta)=C_1-D_1,\quad \kappa\chi(-\delta)=C_3-D_3\ , \quad (26b)$$
$$\kappa\Lambda=A_1+A_1^*=A_3+A_3^*\ ,$$
$$\kappa R=C_1+C_3\ .$$

The loss-gain $\gamma(\delta)$ $(-A_1+B_1)$ and coupling $\chi(\delta)$ (C_1-D_1) coefficients are the correct semiclassical expressions. An immediate comparison of Λ and $A=A_1+A_1^*$ terms is possible for $\Delta_1=0$ (where $A_1=A_3^*$) by comparing Fig. 3 of the Sargent *et al.* paper[46] with Fig. 7(a) of this work. The curves are identical. A comparison of R and $C=C_1+C_3$ is also possible for $\Delta_1=0$ (where $C_3=C_1$) by comparing Fig. 4 of Sargent *et al.*[46] and also figures plotted in Holm and Sargent[52] with Fig. 8 of this paper. Again, exact agreement is obtained. More recently Holm and Sargent[57] have shown analytical agreement between the two theories for the degenerate case $\delta=0$ (for all detunings Δ_1). Further comparisons[58] of the Λ and R noise spectra for nonzero atomic detunings indicate exact agreement for all δ between the two theories.

It is possible to solve for the time-dependent linear Eqs. (19) or (20) and to thus solve for quantities such as the number of photons in each cavity mode and the squeezing in a combined cavity mode. The squeezing is easily determined once one has solved (20) for the quantities $\langle a_2^\dagger a_2\rangle$, $\langle a_3^\dagger a_3\rangle$, and $\langle a_2 a_3\rangle$. The "variance" in the quadrature $X_\theta=a_2e^{-i\theta}+a_3^\dagger e^{i\theta}$ is given by[59,60]

$$V(X_\theta)=1+\langle a_2^\dagger a_2\rangle+\langle a_3^\dagger a_3\rangle+e^{-2i\theta}\langle a_2 a_3\rangle+e^{2i\theta}\langle a_2^\dagger a_3^\dagger\rangle \quad (27a)$$

(once we have noted that $\langle a_2\rangle=\langle a_3\rangle=\cdots=0$) and squeezing is obtained when $V(X_\theta)<1$. This calculation of the internal cavity statistics is the procedure taken in many earlier works[16,17] and by Holm and Sargent.[52]

However, the internal cavity mode differs from the field transmitted through the cavity port and external to the cavity. Unlike the cavity field, the external field is multimode, comprising of traveling waves of different frequencies. Thus we must consider an intensity and squeezing spectrum for the external field. There is a direct proportionality (determined by the cavity parameter κ) between the internal cavity intensity (or squeezing) and the *total* external intensity (or squeezing). However, the individual frequency components of the external field show different intensities and squeezing. It is the transmitted field external to the cavity which is experimentally accessible. These important points were first made by Yurke.[18] He showed that the squeezing in the external field of a single-port cavity and at the sideband frequency $(\omega_L+\epsilon)$

could be perfect. This is in contrast to previous calculations[16,17] on the internal mode which predicted at best 50% squeezing. Yurkes treatment was a single-mode analysis. Collett and Gardiner and co-workers[19,20,26,53] have subsequently developed a theory to calculate the squeezing spectrum of the external field. We use their theory to calculate the statistics of the transmitted field.

IV. SQUEEZING AND INTENSITY SPECTRA OF THE TRANSMITTED FIELD

Of particular relevance to us then is the statistics of the field external to the cavity. Squeezing may be observed in a homodyne detection scheme,[8,25,59,60] where the output sidebands $a_{2,\text{out}}, a_{3,\text{out}}$ at frequencies $\omega_L \pm \epsilon$ beat with a local oscillator $\varepsilon_{\text{LO}} = \varepsilon e^{i\theta_{\text{LO}}}$, phase shifted θ_{LO} with respect to the external driving field at frequency ω_L. The sidebands and local oscillator beat on the surface of a photodetector forming a photocurrent $i(\epsilon)$. A spectrum analyzer allows measurement of the fluctuations in the current $i(\epsilon)$ at ϵ, the spectral fluctuations $\langle i^2(\epsilon)\rangle - \langle i(\epsilon)\rangle^2$ being proportional to the variance $V(X_\theta,\delta)$ in the quadrature phases defined by[59,60]

$$X_\theta = a_{2,\text{out}} e^{-i\theta_{\text{LO}}} + a^\dagger_{3,\text{out}} e^{i\theta_{\text{LO}}} ,$$
$$V(X_\theta,\delta) = \tfrac{1}{2}\langle X_\theta^\dagger X_\theta + X_\theta X_\theta^\dagger\rangle - \langle X_\theta\rangle\langle X_\theta^\dagger\rangle . \tag{27b}$$

Of interest to us then is the spectral fluctuations of the output field.

The Langevin equation (13) describing the cavity modes α_2 and α_3 may be rewritten in the following matrix form:

$$\frac{d}{dt}\boldsymbol{\alpha} = -\underline{A}\boldsymbol{\alpha} + \underline{D}^{1/2}\boldsymbol{\varepsilon}(t) , \tag{28}$$

where $\boldsymbol{\alpha} = (\alpha_2, \alpha_2^\dagger, \alpha_3, \alpha_3^\dagger)$, $\boldsymbol{\varepsilon}(t)$ is a δ-correlated noise force, $\underline{A}$ is the drift matrix derivable from Eq. (13), and $\underline{D}$ is the diffusion matrix whose elements determine the noise correlations (14) as $\langle \Gamma_i(t)\Gamma_j(t')\rangle = D_{ij}\delta(t-t')$.

The semiclassical steady-state solutions are the deterministic solutions derived from the drift term $\underline{A}$ only, ignoring the diffusion $\underline{D}$ completely. The deterministic steady-state solution I for the pump mode ($\delta=0$) is given by the usual optical bistability curve given by Eq. (16). The deterministic steady-state solution and criteria for bistability have been well studied previously, for example, in Refs. (61) and (62). The fluctuations to first order about the steady-state solution I are given by the linear equation (28) with $\delta=0$. The steady-state deterministic solution for the sidebands ($\delta\neq 0$) is

$$\alpha_2^{\text{ss}} = (\alpha_2^{\text{ss}})^\dagger = \alpha_3^{\text{ss}} = (\alpha_3^{\text{ss}})^\dagger = 0 \tag{29}$$

since we have assumed no direct pumping of these modes by an external driving field. The stability of these steady-state deterministic solutions is checked by calculation of the eigenvalues of the drift matrix A. A solution is stable only if these eigenvalues have positive real parts. Alternatively one may use equivalent Hurwitz criteria to derive the following stability conditions:

$$a_1 > 0, \quad h_1 = a_1 a_2 - a_3 > 0 ,$$
$$h_2 = h_1 a_3 - a_1^2 a_4 > 0, \quad a_4 > 0 \tag{30}$$

where

$$a_1 = 2\,\text{Re}[\gamma(\delta)+\gamma(-\delta)] = \text{Tr}\underline{A} ,$$
$$a_2 = 2\,\text{Re}\{[\gamma^*(\delta)\gamma(-\delta) - \chi^*(\delta)\chi(-\delta) + \gamma(\delta)\gamma(-\delta)]\} + |\gamma(-\delta)|^2 + |\gamma(\delta)|^2 ,$$
$$a_3 = 2\,\text{Re}\{[\gamma(\delta)+\gamma^*(-\delta)][\gamma^*(\delta)\gamma(-\delta) - \chi^*(\delta)\chi(-\delta)]\} ,$$
$$a_4 = |\gamma(\delta)\gamma^*(-\delta) - \chi(\delta)\chi^*(-\delta)|^2 = \det\underline{A} .$$

Clearly, the last condition is always satisfied. Parameter regimes where there is not stability of these steady-state solutions are indicated in the figures as dashed lines. For the degenerate situation $\delta=0$, the stability criteria reduce to

$$\gamma_R(0) > 0$$
and
$$|\gamma(0)| > |\chi(0)| . \tag{31}$$

The first condition is always satisfied, the medium absorbing radiation at the pump frequency. We see, however, that as the degenerate coupling coefficient increases sufficiently, unstable regions are possible.

The linear equation (28) with noise $\underline{D}$ included can be solved using standard techniques,[63] enabling calculations of the correlations $C_{ij} = \langle \alpha_i, \alpha_j\rangle = \langle \alpha_i\alpha_j\rangle - \langle \alpha_i\rangle\langle \alpha_j\rangle = \langle \alpha_i\alpha_j\rangle$. We note that since $\langle a_2\rangle = \langle \alpha_2\rangle = \cdots = 0$, $C_{ij} = \langle \alpha_i\alpha_j\rangle$. Although the steady-state deterministic solution for the sidemodes is zero, the $\langle \alpha_2^\dagger\alpha_2\rangle$ of these modes is nonzero because of the presence of the noise $\underline{D}$. We thus get a buildup of photons in the side modes due to spontaneous emission. This buildup is described to first order by our linear equation (28) and its solution C_{ij}. For the case $\delta=0$, the solution represents the first-order correction to the deterministic or coherent solution I. The solution C_{ij} enables quantities such as the mean number of photons and the squeezing in the intracavity modes to be determined.

As discussed above, of more relevance to us given usual experimental situations is the transmitted field external to the cavity and comprised of many frequencies. We consider a fixed sideband frequency $\omega_L + \epsilon$. The linearized expression for the ϵ-fixed spectrum centered at $\omega_L + \epsilon$ (i.e., a frequency ω from $\omega_L + \epsilon$) of the correlation matrix C_{ij} is written[63]

$$S_{ij}(\omega,\delta) = \int_{-\infty}^{\infty} e^{-i\omega t}\langle \alpha_i(t)\alpha_j(0)\rangle dt$$
$$= [(\underline{A} + i\omega I)^{-1}\underline{D}(\underline{A}^T - i\omega I)^{-1}]_{ij} , \tag{31a}$$

where I is the identity matrix. In the high-Q cavity ($\kappa \ll \gamma_\perp$) considered here the δ-fixed spectrum [$S(\omega,\delta)$ as a function of ω] generally has a Lorentzian profile and its width is of order κ. In this work, we restrict attention to the case $\omega=0$. The expression (31a) is valid provided the deterministic steady-state solutions for the pump I and the weak fields are stable, i.e., the criteria given by (29) are satisfied.

The solutions for the elements of the spectrum matrix are

$$S_{12}(0,\delta)=\frac{\{\Lambda[|\gamma(-\delta)|^2+|\chi(\delta)|^2]+R\gamma^*(-\delta)\chi^*(\delta)+R^*\gamma(-\delta)\chi(\delta)\}}{\kappa|\gamma(\delta)\gamma^*(-\delta)-\chi(\delta)\chi^*(-\delta)|^2}=S_{21}(0,\delta)\ ,$$

$$S_{34}(0,\delta)=S_{12}(0,-\delta)=S_{43}(0,\delta)\ ,$$

$$S_{13}(0,\delta)=e^{2i\theta_0}\bar{S}_{13}(0,\delta)=S_{31}(0,\delta)\ , \tag{31b}$$

$$\bar{S}_{13}(0,\delta)=\frac{\{\Lambda[\gamma^*(-\delta)\chi(-\delta)+\gamma^*(\delta)\chi(\delta)]+R\gamma^*(\delta)\gamma(-\delta)+R^*\chi(\delta)\chi(-\delta)\}}{\kappa|\gamma(\delta)\gamma^*(-\delta)-\chi(\delta)\chi^*(-\delta)|^2}\ .$$

The elements $S_{12}(0,\delta)$ and $S_{34}(0,\delta)$ correspond to the intensities at the sidebands, while $S_{13}(0,\delta)$ is the phase-sensitive element responsible for squeezing.

The statistics of the output sideband modes can now be deduced from the boundary conditions at the cavity mirrors.[18,19] We use the theory developed by Collett and Gardiner[19] and Collett and Walls[26] to deduce the external squeezing spectrum in the P representation. The squeezing in the output sideband modes is then determined by the spectral variance ($\theta=\theta_{\rm LO}-\theta_0$)

$$V(X_\theta,\delta)=2\kappa[S_{12}(0,\delta)+S_{34}(0,\delta)+e^{-2i\theta}\bar{S}_{13}(0,\delta)+e^{2i\theta}\bar{S}^*_{13}(0,\delta)]+1\ , \tag{32}$$

where we have taken the optimal situation of a single-port cavity. Given the factor 2κ for going outside the cavity, this solution is analogous to (27a). Squeezing is obtained where $V(X_\theta,\delta)<1$ and perfect squeezing corresponds to $V(X_\theta,\delta)=0$.

The best squeezing is

$$V(X_\theta,\delta)=2\kappa[S_{12}(0,\delta)+S_{34}(0,\delta)-2|\bar{S}_{13}(0,\delta)|]+1 \tag{33}$$

for

$$\cos(2\theta)=\frac{\mathrm{Re}[\bar{S}_{13}(0,\delta)]}{|\bar{S}_{13}(0,\delta)|}$$

and

$$\sin(2\theta)=\frac{\mathrm{Im}[\bar{S}_{13}(0,\delta)]}{|\bar{S}_{13}(0,\delta)|}\ .$$

We abbreviate $S_{21}(0,\delta)$ to $S_{21}(\delta)$ and refer to it as the incoherent intensity spectrum henceforth. We do not include the coherent δ-function contributions in the plots and discussions of the intensity spectrum, for the sake of convenience.

To investigate the physical meaning of the quantity Λ, we consider decoupling the sidebands, so that $\chi(\delta)=R=0$. In this limit, the transmitted intensity $S_{21}(\delta)$ becomes

$$2\kappa S_{21}(\delta)=\frac{2\Lambda}{|\gamma(\delta)|^2}\ .$$

If we have sufficiently low-cavity cooperativity C (large cavity damping κ) then $2\kappa S_{21}(\delta)\to 2\Lambda$. Thus Λ may be thought of as the transmitted fluorescent spectrum for the two-level atoms in the absence of coupling between sidebands. It is phase insensitive, in the sense that in this limit discussed the phase-sensitive spectral element $S_{13}(0,\delta)$ is zero. The variance $V(X_\theta,\delta)$ is thus independent of phase θ and is given by $V(X_\theta,\delta)=1+2\Lambda$ in this limit.

Figure 9 plots the scaled quantity $n/S_{21}(\delta)/I$ for various Δ_1, C, and cavity detunings ϕ and assuming pure radiative damping ($f=1$). Our theory assumes small fluctuations relative to the pump intensity $|\alpha_1^{ss}|^2$, and thus Fig. 9 demonstrates where our theory is likely to break down. If one keeps n_0 large and is not too close to the turning points of the bistability equation (16), where fluctuations are very large, our theory will hold better.

The absorptive case $\Delta_1=0$ is plotted in Fig. 9(a) for $C=20$, sufficient cooperativity to induce bistability of the pump mode I. Below threshold ($I<1.05$) the spectrum is single peaked, the fluctuations increasing as threshold is

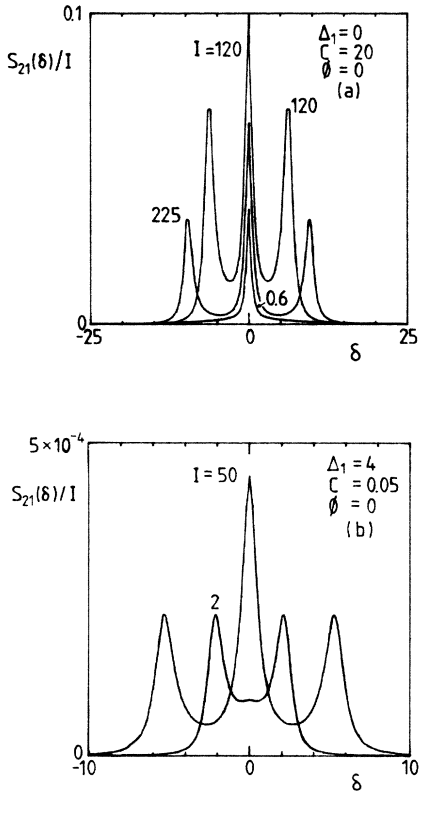

FIG. 9. Plots of the normalized steady-state sideband intensity spectrum $S_{21}(\delta)/I$ transmitted through the cavity. (a) $\Delta_1=0$, $C=20$, $\phi=0$: for steady intracavity pump intensities I corresponding to the upper and lower branch of the bistability curve for I. (b) $\Delta_1=4$, $C=0.05$, $\phi=0$: for high and low pump intensities I.

approached. Way above threshold ($I>225$), the atoms saturate and the curve becomes that of the usual three-peaked resonance fluorescence spectrum. As threshold is approached from above ($I\rightarrow 1$), the sidepeaks move in towards the central peak and their relative height compared to the central peak increases. Such cooperative effects due to the cavity (C,ϕ) have been observed previously in calculations of the transmitted spectrum $S_{21}(\omega,0)$ of the central cavity mode from a low-Q cavity ($\gamma_\perp \gg \kappa$).[64,65]

For $\Delta_1=4$, the plot for low ($2C=1$) cooperativity shows features of usual fluorescence at low intensities, i.e., a doublet is present at the frequencies $\omega_L \pm \Omega$. As one increases the cooperativity C, the doublet along the lower branch disappears. Regardless of C, the usual three-peaked spectrum, with Rabi sidepeaks at Ω, appears far enough above threshold. Nearer threshold, the sidepeaks move into towards the central peak, with a change in relative peak heights. Similar features are exhibited at higher detunings $\Delta_1=100$.

V. DISCUSSION OF SQUEEZING SPECTRA

A. Revision of degenerate $\delta=0$ results

The key question is what orders of magnitude are required for experimental parameters (Δ_1, δ, $2C$, f, and I) to obtain the best possible squeezing. The recent studies by Reid and Walls of degenerate four-wave mixing[24] and optical bistability[27] in a two-level medium pointed to at least three important physical effects which may limit the squeezing possible: the degree of collisional dephasing f, the absorption $\gamma_R(\delta)$, and phase-insensitive fluorescence Λ. We take the value $f=1$, no collisions, in this work. The general principle is then to enhance the nonlinear phase-sensitive process $\chi(\delta)$ and R over the dephasing absorption $\gamma_R(\delta)$ and fluorescence Λ terms. This is done, for example, mathematically in the idealized Hamiltonian (22) and consequent equations, for which $\Lambda=\gamma_R(\delta)=R_R=\chi_R(\delta)=0$ and $R_I=\chi_I(\delta)$. This idealized Hamiltonian for the degenerate $\delta=0$ situation in a ring cavity corresponds to that of idealized dispersive optical bistability:

$$H=\hbar\omega_1 a_1^\dagger a_1+\hbar\chi(a_1^\dagger)^2 a_1^2+i\hbar(a_1^\dagger E e^{-i\omega_L t}-a_1 E^* e^{i\omega_L t}) +a_1\Gamma_c^\dagger+a_1^\dagger\Gamma_c \ . \tag{34}$$

This system was studied by Collett and Walls[26] and shown to give perfect squeezing (in a linear theory of fluctuations as described above) as one approached the turning points of the dispersive optical bistability curve.[64] Squeezing via dispersive optical bistability in a high-Q cavity in a two-level atomic medium, thus incorporating effects of absorption and spontaneous emission not included in (34), was studied by Reid and Walls.[27] The effect of absorption was shown to be significant at low intensities ($I \lesssim \Delta_1$) and high-C values ($2C \gtrsim \Delta_1^2$). The effect of desqueezing fluorescence Λ was important at higher intensities I as one began to saturate the atom ($I\sim\Delta_1^2$). Thus one required sufficient intensity I to attain significant nonlinearity [$\chi(0)\sim 2CI/\Delta_1^3$] so that the turning points of the bistability equations are approached and to overcome the effects of absorption γ_R. Yet the intensity I must be significantly less than the saturation intensity $I_s\sim\Delta_1^2$, so that $\Lambda \ll |\chi(0)|$. (In fact, one needs $I^2 \ll \Delta_1^3$ to ensure this.) These effects are seen by examining the plots of quantities $\gamma_R(\delta)$, $\chi(\delta)$, and Λ at $\delta=0$.

Thus for the degenerate situation $\delta=0$ excellent squeezing is obtainable only for a restricted range of parameters and is thus not experimentally advantageous. One needs high atomic detunings $\Delta_1>10^3$ and thus high C values ($2C>\Delta_1$) and intensities ($I>\Delta_1$) to attain sufficient $\chi(0)$. The squeezing is also sensitive to changes from the optimal values of C and I. Importantly, sensitivity of squeezing to ϕ is noted. The cavity detuning ϕ changes the shape of the bistability curve. The optimal ϕ for squeezing in the degenerate situation corresponded to the transition to bistable behavior where one has a point of inflexion in the bistability curve. Considering the situation $\Delta_1\phi>0$, this value is $\phi\sim 2C/\Delta_1$ (in the high Δ_1 and C limit). This corresponds to the pump resonant with the linear dressed cavity, for which the cavity resonance is shifted due to the refractive index term $\gamma_I(0)$ of the atoms. Decreasing ϕ, one attains clear bistable behavior, but the turning points of the bistable curve are at higher intensity values I. In the degenerate situation the higher intracavity pump intensity I induces fluorescence Λ and squeezing is diminished in the normal bistable situation.

B. Advantages of nondegenerate operation

An insight into the particular difficulties of the degenerate situation is gained by considering the fluorescence spectrum Λ. As discussed above, the fluorescence Λ is phase insensitive and destroys squeezing. The degenerate situation corresponds to the center $\delta=0$ of the spectrum, displayed in Fig. 7. At low intensities I far below saturation the spectrum for a detuned atom is a doublet at the Rabi frequencies. The fluorescence Λ at the center is negligible. As one increases the intensity I towards saturation, however, the center $\delta=0$ resonance fluorescence peak becomes significant. An examination of the plot of Λ (Fig. 7) for higher I shows the fluorescence to be most significant at the center peak, and hence the above-mentioned difficulties of degenerate four-wave mixing. The central fluorescence peak has a finite width of order $\gamma_\perp$. Thus if one increases the sideband detuning ϵ to orders greater than $\gamma_\perp$, we may expect the nondegenerate situation to be less sensitive to the desqueezing effects of fluorescence (spontaneous emission). However, what is relevant in determining the detrimental effect to squeezing of spontaneous emission is the *relative* size of the fluorescence Λ to the four-wave-mixing coupling $|\chi(\delta)|$ (or R) which is responsible for the squeezing.

Thus it becomes instructive to compare the coupling $\chi(\delta)$ (Fig. 6) with the fluorescent spectrum Λ (Fig. 7). This is done for the high-detuning $\Delta_1=100$ case. As described above, at high intensities the fluorescence Λ becomes a three-peaked spectrum resembling that of usual fluorescence. The peaks are at the Rabi frequencies and the central pump ($\delta=0$) frequency, with width $\sim\gamma_\perp$. The coupling spectrum $|\chi(\delta)|$ [or $|R(\delta)|$] shows strong enhancement at the Rabi frequencies, due to the scattering process depicted in Fig. 3. One sees in the coupling spectrum (as compared to the fluorescence Λ spectrum) a still

quite strong enhancement coupling for frequencies between the Rabi peaks. Also, the width of the side peaks in the coupling spectrum is much greater than the width of the peaks in the fluorescence spectrum. Also, because $\chi(\delta)$ represents a coupling between four photons, there is not a significant central peak ($\delta=0$) as in the fluorescence Λ spectrum which relates to emission of single photons. The coupling spectrum is essentially flat and significant [$\chi(\delta)\sim\chi(0)\sim 2CI/\Delta_1^3$ in this region provided $\Delta_1\gg 1$] for regions between the Rabi peaks. Thus one enhances the four-wave-mixing coupling relative to the desqueezing fluorescence by increasing the sideband detuning ϵ over orders of $\gamma_\perp$ so that the fluorescence falls off appreciably from its central fluorescent peak value.

Thus one may expect to totally saturate the atoms and yet avoid the desqueezing effects associated with spontaneous emission by increasing δ appropriately. The consequence of this is that good squeezing becomes possible at much lower detunings Δ_1, lower cooperativity C values, and for a wider range of parameters Δ_1 C, I, and ϕ than is possible in the degenerate situation.

The statistics of the transmitted field is a function not only of the weak field detuning δ and pump intensity I [as described by Λ, $\chi(\delta)$ etc.], but also of the cavity parameters C, the cavity cooperativity, and ϕ the cavity detuning. Collective effects due to the cavity, for example, are apparent in the intensity spectra illustrated in Fig. 9. To study the effect of C and ϕ on the squeezing possible, we consider three different situations corresponding to different choices of ϕ as a function of intensity I: (i) no imaginary components to $\gamma(\delta)$; (ii) $\phi=-\gamma_I(0)$, the external driving field kept approximately resonant with the dressed cavity; (iii) $\phi=$const, the external driving field has a constant frequency. This is the usual situation of optical bistability experiments. We discuss these cases separately.

(i) *Perfect phase matching:* No imaginary component to $\gamma(\delta)$. The simplest situation to consider analytically is where one has no imaginary component to $\gamma(\delta)$ and $\gamma(-\delta)$. The term $\gamma_I(\delta)$ contributes to the refractive index for the field at frequency δ, i.e., gives a change in refractive index due to the two-level atomic medium. It is nonlinear in the pump intensity, including the effect of saturation of the medium. Because of the asymmetry of the dispersion term $\gamma_I(\delta)$ [i.e., $\gamma_I(\delta)\neq\gamma_I(-\delta)$] plotted in Fig. 5, the situation (i) discussed cannot be achieved in the collinear cavity configurations depicted in Figs. 1 and 15. Such perfect phase matching may be possible however if one introduces slightly different directions for the κ vectors of the three fields.

Such considerations are usually more relevant where one has the three waves propagating through the medium, with no cavity.[44] This would pertain to experiments of the type being performed by Bondurant *et al.*[6] However, we restrict our attention in this paper to cavity rather than propagating modes. Thus this situation (i) is not the most relevant experimentally, and we consider it only because of its analytical simplicity.

The main considerations in obtaining good squeezing, for this situation (i), is to obtain sufficient nonlinearity so that the threshold (instability) is approached while still avoiding the dephasing effects of absorption $\gamma_R(\delta)$ and fluorescence Λ. With the imaginary components of $\gamma(\delta)$ zero, the criteria at $\delta=0$ for threshold becomes $|\chi(0)|=1+\gamma_R(0)$. One has stability where $|\chi(0)|<1+\gamma_R(0)$.

Figure 10(a) plots the spectrum for squeezing $V(X_\theta,\delta)$ for $\Delta_1=100$, $C=250$, and for various intensities. This value for C is low in the sense that to approach the threshold $|\chi(0)|\sim 1$, one needs high pump intensities $I\sim 3000$, approaching the saturation intensity $I\sim 10^4$. Also, the atomic absorption near $\delta=0[\gamma_R(0)\sim 2C/\Delta_1^2\sim 0.05]$ is insignificant compared to the cavity loss. The reader is reminded of the Figs. 4, 6, and 7 illustrating the absorption $\gamma_R(\delta)$, coupling $\chi(\delta)$, and fluorescence Λ spectra. For intensities of the order $I=3000$, the fluorescence at $\delta=0$ is significant and no squeezing is obtained. Upon increasing $\delta\rightarrow 30$, the fluorescence tails off but the coupling and absorption are flat: $|\chi(\delta)|\sim 2CI/\Delta_1^3$, $\gamma_R(\delta)\sim 2C/\Delta_1^2$. With both the absorption and fluorescence being insignificant and the coupling significant, good squeezing is attained. As one approaches the Rabi frequency $\delta\rightarrow 50$, however, the squeezing is destroyed. A comparison of Figs. 4, 6, and 7 reveal that the coupling sidepeak is broader than the absorption and fluorescence sidepeaks. Thus as $\delta\gtrsim 40$, the coupling increases and a broad region of instability is reached. Well above the Rabi frequency, the nonlinearity $\chi(\delta)$ de-

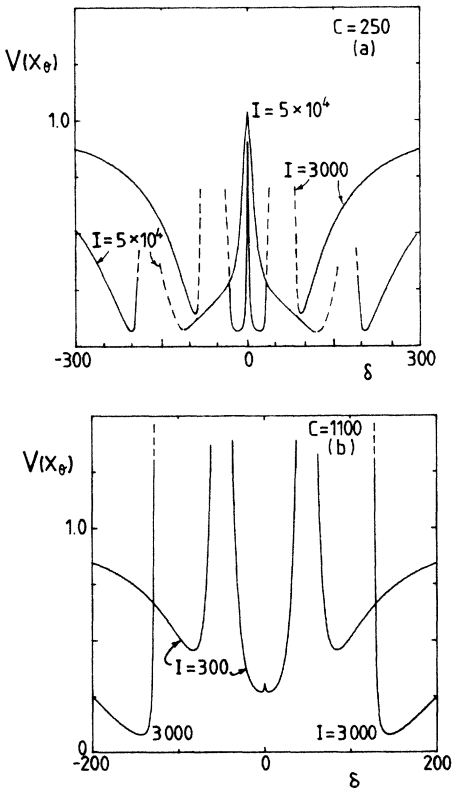

FIG. 10. Plots of the squeezing spectrum $V(X_\theta,\delta)$ of the transmitted field for various pump intensities I: Ignoring the imaginary component of $\gamma(\delta)$, i.e., ignoring dispersion: $\Delta_1=100$. Dashed curves correspond to unstable solutions. (a) $C=250$: The Rabi frequency for $I=3000$ is $\delta=63$, and for $I=5\times 10^4$ is $\delta=165$. (b) $C=1100$.

creases and another stable region is obtained. Good squeezing is obtainable initially but decreases as δ increases and the nonlinearity falls away. At higher intensities I, the Rabi frequency increases. The squeezing spectrum however shows similar behavior.

The second plot Fig. 10(b) shows the squeezing spectrum for a higher C value, $C=1100$. In this case, the nonlinearity is significant for lower intensities, $I\sim 300$. Here a central $\delta=0$ fluorescence peak is nonexistent, and the squeezing at $\delta=0$ is limited only by the absorption $(2C/\Delta_1^2\sim 0.22)$. A reasonable amount of squeezing is obtainable at $\delta=0$, for $I=300$. Since the central fluorescence is not present to destroy squeezing at $\delta\sim 0$, there is *no* significant improvement in the squeezing upon increasing the detuning δ. In fact, as δ approaches the Rabi frequency, the absorption γ_R increases significantly relative to χ, and destroys the squeezing. The effect of the absorption peak is particularly pronounced at lower intensities (see Fig. 4). Stability is maintained since $1+\gamma_R(\delta)>|\chi(\delta)|$. As δ is increased beyond the absorption Rabi sidepeaks, squeezing improves for a small regime of δ. However, the nonlinearity then tails off, and squeezing disappears. At higher intensities, the coupling at $\delta=0$ increases (see Fig. 6) and the solutions are unstable. Stable solutions are possible, at higher intensities, only by increasing δ sufficiently to reduce the nonlinear coupling.

The results discussed above have been presented previously by Reid and Walls.[49]

(ii) $\phi=-\gamma_I(0)$. The second situation we consider is where the external pump frequency ω_L is adjusted at various intensities so that it is kept approximately resonant with the nonlinear dressed pump cavity. $\gamma_I(0)$ relates to the change in refractive index term due to the two-level atomic medium for the pump frequency $\delta=0$. This would seem to be the most straightforward way of maximizing the response of the internal cavity field to the external driving field.

The squeezing spectrum $V(X_\theta,\delta)$ is plotted in Fig. 11. We see that for δ much less than the Rabi frequency, the spectrum $\gamma_I(\delta)$ shown in Fig. 5(c) is relatively flat. Thus for this regime of small δ up to the Rabi frequency, the imaginary component of $\gamma(\delta)$ in Eq. (13) is essentially zero (that is, the pump is close to resonance with the dressed cavity) and the squeezing is similar to that discussed above in (i). For example, we see for the case $C=250$, $I=3000$ [Fig. 11(a)] significant improvement in squeezing by increasing δ from $\delta=0$ to $\delta=30$ and thus avoiding the central fluorescence Λ peak. As one approaches the Rabi frequency $\delta\rightarrow\frac{1}{2}(2I+\Delta_1^2)^{1/2}$, however, the term $\gamma_I(\delta)$ differs significantly from $\gamma_I(0)$. There are thus important changes [compared to (i)] in behavior in the regime of δ near the Rabi frequency.

At low intensities ($I<\Delta_1^2$) the absorption becomes large in the vicinity of the Rabi frequency and the squeezing is reduced [$V(X_\theta,\Delta)\rightarrow 1$] upon approaching the Rabi frequency [as in (i)]. However, comparison of Figs. 11 and 10 reveal that the variance V is not so great when the dispersion is included, tending toward the coherent value obtained with no medium. Also, the region of instability about the Rabi frequency has narrowed. At higher δ, the

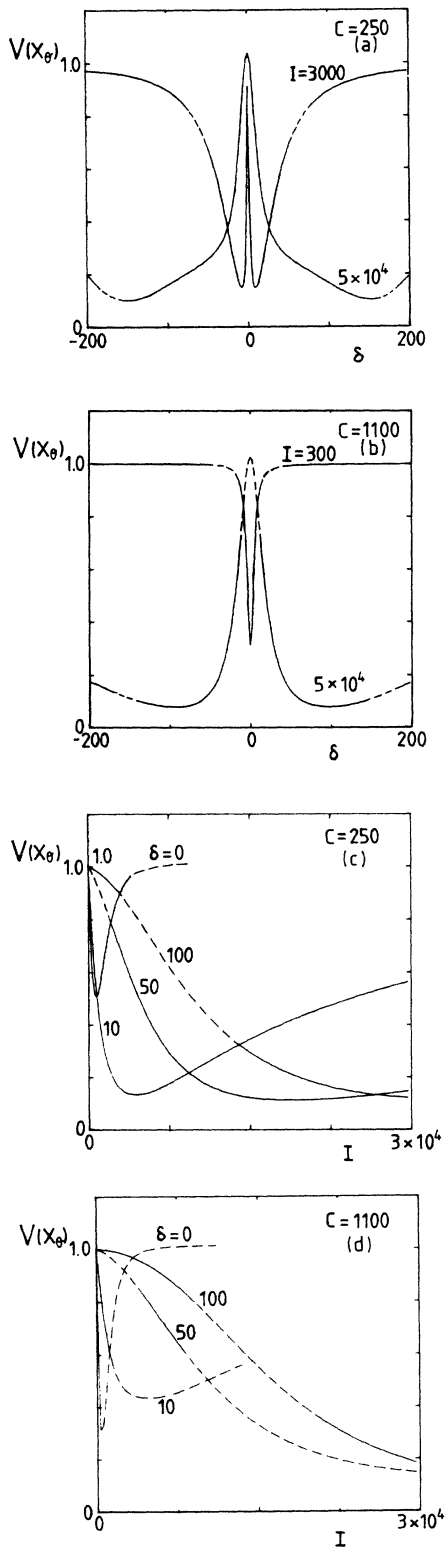

FIG. 11. Transmitted squeezing $V(X_\theta,\delta)$ where the cavity detuning ϕ is such that approximate resonance is maintained at all intensities between the external pump and the nonlinear cavity, $\phi=-\gamma_I(0)$. Dashed curves are unstable regions $\Delta_1=100$. Plots of $V(X_\theta,\delta)$ versus δ for various I: (a) $C=250$: The Rabi frequency for $I=3000$ is $\delta=63$ and for $I=5\times 10^4$ is $\delta=165$. (b) $C=1100$. Plots of $V(X_\theta,\delta)$ versus I for various δ: (c) $C=250$, (d) $C=1100$.

variance remains close to the coherent limit [$V(X_\theta,\delta)\rightarrow 1$], the nonlinearity reducing.

At higher intensities I (at least of the order of the saturation intensity $I=\Delta_1^2$) there is the possibility of good squeezing for large stable regions of δ near the Rabi frequency $\delta=\frac{1}{2}(2I+\Delta_1^2)^{1/2}$. The orders of magnitude of the absorption (or gain) $\gamma_R(\delta)$ and dispersion $\gamma_I(\delta)$ terms drop off more quickly with increasing intensity than the coupling $|\chi(\delta)|$. The presence of the $\gamma_I(\delta)$ results in much smaller (sometimes nonexistent) regions of instability about the Rabi frequency, compared to case (i) in the preceding. Figure 11 illustrates this feature of good squeezing possible at very high intensities well above saturation and for sufficient detuning δ. One can also obtain in principle good squeezing for the situation of very high-C values ($C=8000$) provided the intensity I (and thus δ) is increased sufficiently. The higher intensities are necessary to reduce (through saturation) the absorption $\gamma_R(\delta)$ sufficiently. Squeezing is not significant in these high-C ($2C>\Delta_1^2$) examples for low intensities below saturation levels ($I\lesssim\Delta_1^2$) because of the then dominance of atomic absorption $\gamma_R(\delta)\sim 2C/\Delta_1^2$. Since high-$I$ values are involved to get the good squeezing, however, it would appear more practical to employ lower C values. This is provided sufficient nonlinear coupling $\chi(\delta)$ can be obtained before the onset of saturation.

For the high intensity examples, it is possible to get good squeezing precisely at the Rabi frequency (provided the solution is stable). It is thus interesting to compare the various terms $\gamma_R(\delta)$, $\gamma_I(\delta)$, $\chi(\delta)$, R, and Λ in this region where there is good squeezing. As one approaches the Rabi frequency, one finds the medium is acting as the ideal four-wave mixer described by Hamiltonians (34) and (22), i.e., the nonlinear coupling $\chi(\delta)$ and R are significant [compared to the cavity loss $-|\chi(\delta)|\sim 1$] and almost pure imaginary, while the absorption and fluorescence terms are relatively small. This is possible because of the broader widths of the coupling sidepeaks as compared to the fluorescent sidepeaks Λ, χ_R, and R_R. Precisely at the Rabi frequencies, however, the terms Λ, R_R, γ_R, γ_I, and χ_R are the same order of magnitude as R_I,χ_I. The behavior of the two-level atom at the Rabi frequency is no longer that of the dispersive ideal four-wave mixer [Hamiltonian (22)]. Yet excellent squeezing is predicted possible at the Rabi frequencies for a two-level atom for atoms well saturated. This is an interesting example of phase-sensitive fluorescence. We conclude that the atomic fluorescence transmitted through the cavity at high intensities is phase insensitive (destroys squeezing) at the center peak but phase sensitive at the side peaks. This is not surprising in physical terms in view of the strong enhancement of coupling possible between sidemodes detuned from the pump by the Rabi frequency [Fig. 3(b)]. There is resonance with the energy levels of the dressed atom and the process is thus different from the dispersive processes [for example, Hamiltonians (22) and (34)] normally considered for squeezing. The real components χ_R, R_R, and γ_R becoming significant and playing an important role in the squeezing.

Figures 11(c) and 11(d) illustrate the squeezing spectrum $V(X_\theta,\delta)$ versus the intracavity pump intensity I (for various δ). It is apparent from these plots that nondegenerate four-wave mixing is particularly advantageous for the low-C situation [$C=250$, Fig. 11(c)] where significant improvement in squeezing is possible at lower intensities I (and thus for lower δ values, $|\delta|<|\Delta_1|/2$). This is compared to the result for higher C values [$C=1100$, Fig. 11(d)] where nondegenerate four-wave mixing is advantageous only at very high intensities, well above the saturation intensity (and thus for high-δ values). This point has been made in Ref. 49.

(iii) *ϕ constant.* The alternative situation we consider is where the driving field is kept at a constant frequency, i.e., the cavity detuning ϕ is fixed at a constant. We study two possibilities: firstly where $\phi\sim 2C/\Delta_1$ and secondly $\phi=0$. The situation of fixed ϕ corresponds to that of usual optical bistability (Fig. 1).

$\phi\sim 2C/\Delta_1$. Here we are selecting the external driving field to be approximately in resonance with the linear or low intensity dressed pump cavity. The term $\gamma_I(0)$ is of the order $2C/\Delta_1$ for low intensities I well below the saturation intensity. Thus the squeezing spectrum for $\phi\sim 2C/\Delta_1$ at low intensities I [Fig. 12(a)] coincides with that of (ii) $\phi=-\gamma_I(0)$ (Fig. 11). The best squeezing occurs near $\delta=0$ and is diminished approaching and beyond the Rabi frequencies.

At higher intensities approaching and exceeding the saturation intensity [Fig. 12(c)], there is a distinction between $\gamma_I(0)$ and $2C/\Delta_1^2$ and thus a considerable detuning between dressed cavity and pump. The spectrum is no longer that of $\phi=-\gamma_I(0)$. At $\delta=0$ the squeezing spectrum reflects the central fluorescence peak. Upon increasing δ beyond this peak, however, the squeezing does not improve as readily as in the example (ii) where $\phi=-\gamma_I(0)$ and where the driving field is resonant with the dressed cavity. The detuning between driving field and cavity reduces the squeezing possible. Upon approaching the Rabi sidepeak of the coupling spectrum $\chi(\delta)$, the squeezing improves more significantly.

Regimes of instability appear at or beyond the Rabi frequency. As δ increases beyond the coupling sidepeak, the squeezing drops sharply. Thus we have narrow squeezing peaks centered at the Rabi frequency. The best squeezing obtainable at these higher intensities is less than that possible in the case (ii) discussed above where the driving field is resonant with the pump cavity.

Figure 12(d) plots the squeezing as a function of intensity I for $C=1100$. For $\delta=0$ there is an intermediate regime of I for which instability appears. In fact, this situation shows optical bistability of the intracavity intensity I with the external driving field intensity. The lower stable intensity regime of I corresponds to the lower branch of the optical bistability curve and the higher stable I values to the upper branch. As discussed previously in Sec. V A, $\phi\sim 2C/\Delta_1$ represents the transition to bistable behavior for the pump mode. As ϕ decreases, bistability is more pronounced but one requires higher intensities I to reach the unstable regime. Figure 12(d) illustrates that the squeezing at higher δ corresponds to the upper branch of the bistability curve.

Figures 12(a), 12(b), and 12(c) illustrate not only the squeezing spectrum but also the intensity spectrum

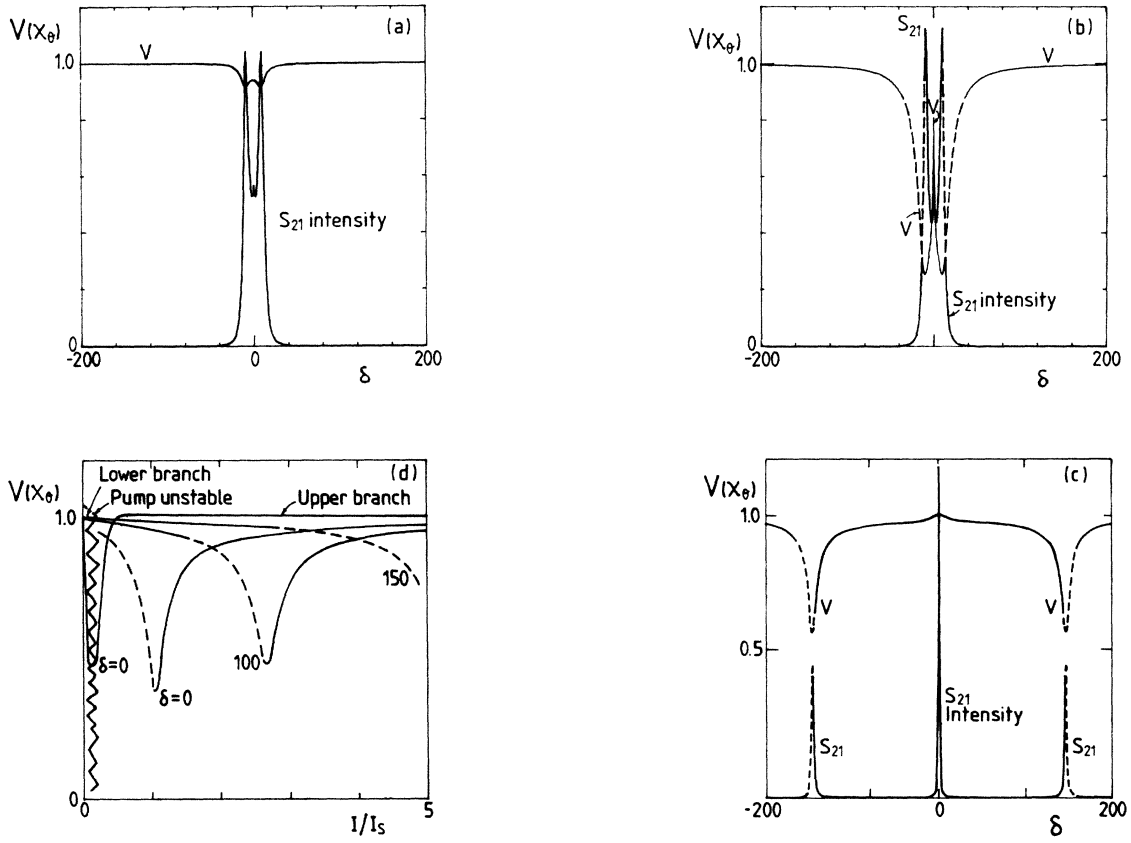

FIG. 12. The transmitted squeezing $V(X_\theta,\delta)$ for fixed cavity detuning ϕ chosen so that the external pump is near resonance with the cavity at low intensities I insufficient to saturate the atoms. $\Delta_1=100$, $C=1100$, $\phi=19$. The transmitted squeezing $V(X_\theta,\delta)$ and intensity $S_{21}(\delta)/I$ spectra: (a) $I=100$: low intensity corresponding to the lower branch of the bistability curve for the pump mode. (b) $I=3000$: moderate intensity corresponding to the upper branch of the bistability curve, but near to the region of instability. (c) $I=5\times10^4$: high intensity corresponding to upper branch of the bistability curve for the pump, and atoms well saturated. (d) Squeezing $V(X_\theta,\delta)$ versus the intracavity pump intensity in units of the saturation intensity $I_s=\Delta_1^2=10^4$. $\phi=18$.

$S_{12}(\delta)$, for various intensities. The plot for high intensity $I=5\times10^4$ corresponds to well above the region of bistability, on the upper branch. We see that the intensity spectrum for the saturated atoms is three peaked similar to that of usual resonance fluorescence: a center peak and two Rabi sidepeaks at the Rabi frequencies. Comparison with the squeezing spectrum show it too is three peaked: the center peak destroys the squeezing and the Rabi sidepeaks are squeezed peaks. The squeezing is destroyed at the center peak due to the dephasing central resonance fluorescence peak and is enhanced at the sidepeaks due to the enhancement of four-wave-mixing coupling. At such high intensities, the atoms are well saturated and do not exhibit collective effects possible at lower intensities. We point out also that the intensity spectra calculated here are similar to transmitted spectra calculated from a single-mode low-Q ($\gamma_\perp \gg \kappa$) cavity.[65,66]

The intensity is reduced in Fig. 12(b) to $I=3000$, corresponding to the upper branch but closer to the region of instability. The intensity sidepeaks now move in closer to the center peak. These peaks coincide to the peaks (or dips) in the squeezing spectrum. This shifting of the sidepeaks has been observed in the low-Q cavity intensity and is, along with other features such as linewidth narrowing near the instable region, a cooperative effect possible where one has many atoms.

In Fig. 12(a) we reduce the intensity further, to a point on the lower branch. The intensity spectrum becomes a doublet. The intensity and squeezing spectrum now have no center peak, the central fluorescence Λ peak vanishes at low intensities. Hence when looking at the squeezing spectrum for low I, we see no significant reduction in squeezing for $\delta=0$. The nondegenerate and degenerate results are thus much the same in this low intensity regime. At such low intensities the nonlinearity $|\chi(\delta)|$ of the cavity is reduced [$|\chi(\delta)|<1$] and the squeezing is also reduced.

We notice that the widths of the squeezing and intensity peaks for this case of $\phi\sim 2C/\Delta_1$ are relatively narrow compared to spectral shape possible for $\phi=-\gamma_I(0)$ and is determined essentially by the width of the coupling Rabi sidepeak (Fig. 6). Also, the best squeezing is obtained for this case of $\phi\sim 2C/\Delta_1$ at low intensities less than the saturation intensity ($I<\Delta_1^2$). This is not surprising given

that the choice of ϕ brings the driving field closer to the resonance with the linear pump cavity and is out of resonance at higher intensities saturating the atoms.

$\phi < 2C/\Delta_1$; $\phi \to 0$. It is possible to broaden the width of the squeezing peaks and obtain better squeezing at higher intensities $I > \Delta_1^2$ by decreasing ϕ. The dispersive term $\gamma_I(\delta)$ decreases for such high intensities and thus by decreasing ϕ we bring the driving field closer to resonance with the nonlinear dressed high intensity cavity.

These effects are shown in Figs. 13. The squeezing is as expected reduced for lower intensities below the saturation intensity $I < \Delta_1^2$, but improved for higher intensities $I > \Delta_1^2$. As $\phi \to 0$ [Fig. 13(b)], the intensity at which best squeezing occurs, and the squeezing obtainable, increases. Since the intensities are well above saturation levels, the absorption $\gamma_R(\delta)$ becomes negligible, apart from small resonances at the Rabi frequencies. Good squeezing is possible here because the absorption term (Fig. 4) is more sensitive to saturation than the coupling term (Fig. 6).

The squeezing spectrum for $\phi = 0$ [Fig. 13(b)] for the high intensities is thus similar to that obtained at high intensities for $\phi = -\gamma_I(0)$ [Fig. 11(b)]. We see [as was the case in $\phi = -\gamma_I(0)$] in Fig. 13(b) for $\phi = 0$ that very good squeezing is possible at high intensities saturating the atoms for stable regimes near the Rabi frequency. Also plotted in Fig. 13(b) is the intensity spectrum showing again that the squeezing peaks coincide with the intensity sidepeaks. Figure 13(c) plots the squeezing spectrum for $I = 5 \times 10^4$ and for various ϕ at the lower C value 250. We see how the width of the squeezing peak has

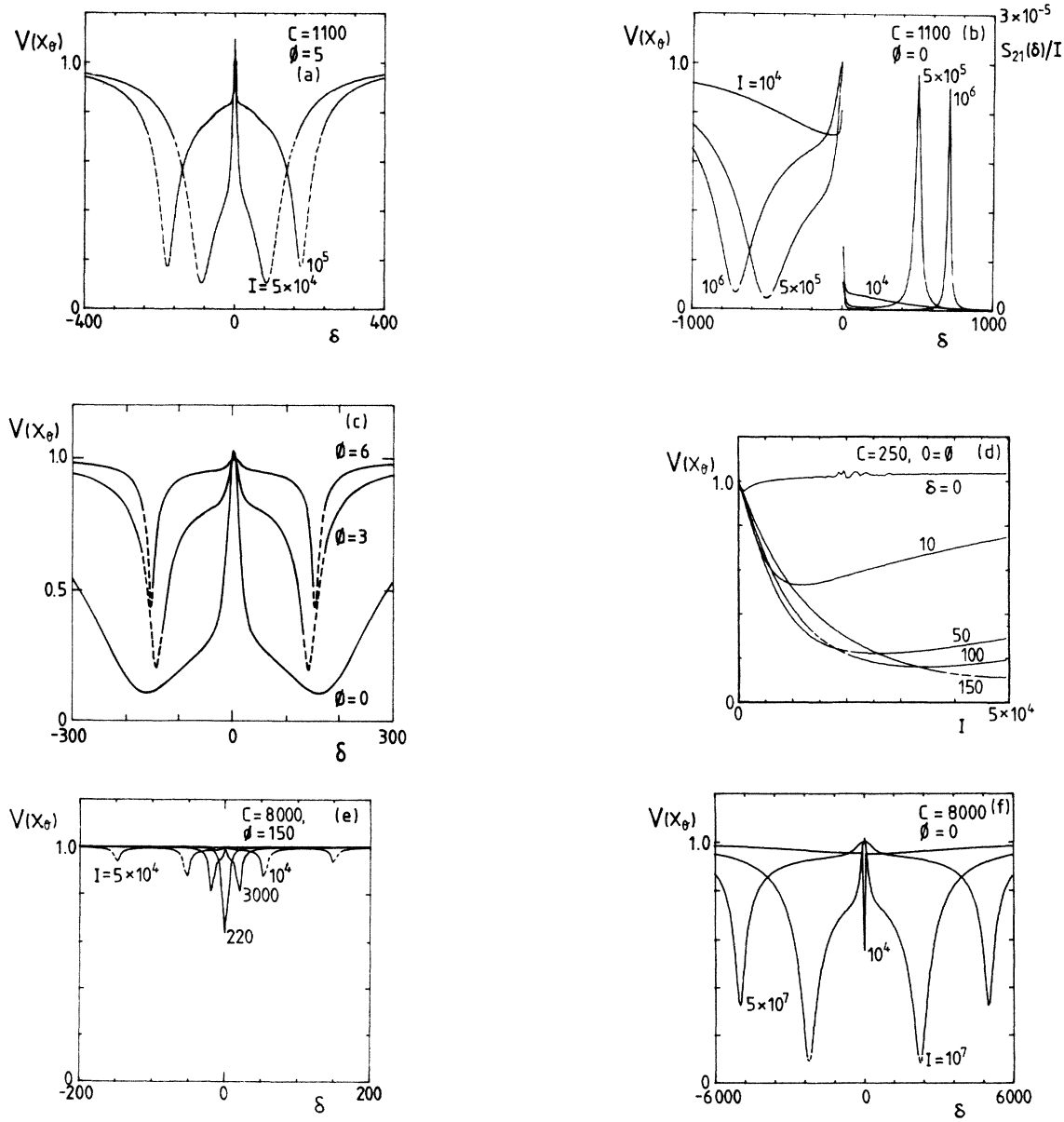

FIG. 13. Transmitted squeezing $V(X_\theta, \delta)$: $\Delta_1 = 100$. (a) $\phi = 5$, $C = 1100$. Rabi frequency for $I = 5 \times 10^4$ is $\delta = 165$ and for $I = 10^5$ is $\delta = 230$. (b) $\phi = 0$, $C = 1100$. Rabi frequency for $I = 5 \times 10^5$ is $\delta = 502$ and for $I = 10^6$ is $\delta = 708$. (c) $I = 5 \times 10^4$, well-saturated atoms, $C = 250$. Rabi frequency is $\delta = 165$. (d) $\phi = 0$, $C = 250$. Squeezing $V(X_\theta, \delta)$ versus I. (e) $C = 8000$, $\phi = 150$. (f) $C = 8000$, $\phi = 0$. Rabi frequency for $I = 10^7$ is $\delta = 2237$.

broadened on decreasing ϕ, due to the greater range δ for which the driving field is approximately resonant with the dressed cavity.

Comparison of Figs. 13(b) and 13(c) illustrate that one can increase the cooperativity or C value (and hence the linear atomic absorption at $\delta=0$) and still obtain excellent squeezing. However greater intensities (well above saturation) are needed in order to reduce the absorption $\gamma_R(\delta)$ sufficiently. The excellent squeezing becomes possible for $\phi\sim 0$ (to bring the cavity into resonance) and in the regime of δ around the Rabi frequency $\delta\sim\frac{1}{2}(2I+\Delta_1^2)^{1/2}$. For example, with $C=8000$ and $\phi\sim 2C/\Delta_1=150$, only a small amount of squeezing is possible [Fig. 13(e)]. Yet excellent squeezing is possible for $C=8000$, $\phi=0$ and $I=10^7$ [Fig. 13(f)]. It is pointed out and is apparent from Fig. 13(d) that the excellent squeezing does occur for an optimal range of intensity I. Increasing I beyond this range will result in further saturation of the nonlinear coupling term $\chi(\delta)$ until it becomes small compared to the linearity of the cavity [i.e., $|\chi(\delta)| \ll 1$].

Another implication of nondegenerate four-wave mixing is that one can attain good squeezing at much lower atomic detunings Δ_1 and hence much lower C and I values. The squeezing spectrum is plotted in Fig. 14 for an atomic detuning $\Delta_1=4$. The first plot 14(a) is for sufficient cooperativity $C=20$ that the pump mode is clearly bistable. The intensity $I=10$ corresponds to the lower branch and $I=500$ to the upper branch. The intensity spectra are also plotted, showing transition from a single broader peak at the low intensity to the three-peaked triplet at the higher intensity. For the higher intensity where atoms are well saturated, significant squeezing is obtainable at the sidepeaks, even for this low value of atomic detuning. We note significant increase in noise (well above the coherent level) corresponding to the central fluorescence peak.

The second plot 14(b) is for a much lower C value ($C=5$), not quite sufficient to enable bistability of the pump. We see still significant squeezing obtainable at the Rabi sidepeaks for well-saturated atoms. This is analogous to the situation $C=250$ in the case $\Delta_1=100$ discussed in the preceding. Lowering the cooperativity value C much further, however, significantly reduces the nonlinearity, and hence the squeezing obtainable before the onset of saturation.

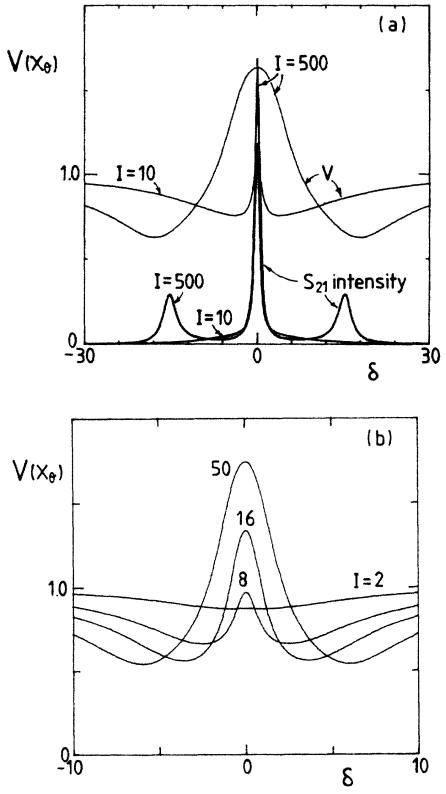

FIG. 14. Good squeezing is possible for low atomic detunings: $\Delta_1=4$, $\phi=0$. (a) $C=20$, (b) $C=5$.

VI. COMPARISON OF EXPERIMENTAL OBSERVATIONS OF SQUEEZING WITH THEORY

The recent work of Slusher *et al.*[12] has reported the experimental observation of squeezed light. In this section we make a comparison of the experiment with the theory presented in this paper, making clear approximations calculated.

The experiment (Fig. 15) utilizes a nondegenerate four-wave-mixing scheme with an atomic beam of sodium as the nonlinear mixing medium. A laser field at frequency ω_L is injected into a pump cavity of resonance frequency ω_1 and forms an intracavity pump mode. The pump laser is tuned near the sodium D_2 resonance ω_0. Shifted at a small angle to the pump cavity is a second single-port squeezing cavity with two sideband cavity modes separated in frequency from the pump cavity mode ω_1 by $\pm\Delta\omega$. Mixing of the pump and the sideband modes occurs via the nonlinear medium and squeezing is observed in the output of the squeezing cavity near the sideband frequencies $\omega_L\pm\Delta\omega$.

A useful model for the sodium is a two-level atom with resonance frequency ω_0. A quantum-mechanical theory of the two-level atomic medium which calculates the squeezing in the output cavity field, for nondegenerate four-wave mixing, is presented above. The calculations apply to a high-Q ring cavity. The approximation is made that one can neglect spatial fluctuations and this is assumed valid for highly reflecting cavity mirrors. A

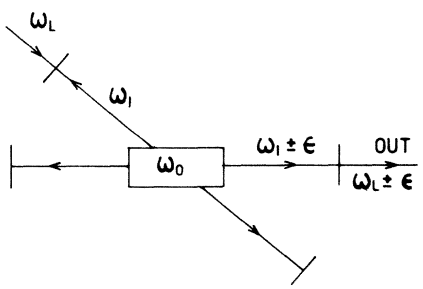

FIG. 15. Diagram of nondegenerate four-wave mixing in a standing-wave cavity.

modification of the results above for the ring cavity is made to better describe the standing-wave cavity mode of the Slusher *et al.* experiment. We take the simplest mode function [$u_j(r)=\sqrt{2/V}\sin(\mathbf{k}_j\cdot\mathbf{r})$; $j=1,2,3$, and where V is the cavity volume] and calculate averages over the standing-wave phase.

For example, the equation (13a) for the pump standing-wave cavity mode is rewritten

$$\dot{\alpha}_1=E-\kappa_1(1+i\phi_1)\alpha_1-\frac{2\kappa_1C_1\alpha_1}{1+i\Delta_1}\int_V\frac{u_1(r)}{\Pi(0)}d^3r$$

$$\rightarrow E-\kappa_1(1+i\phi_1)\alpha_1$$

$$-\frac{2\kappa_1C_1\alpha_1}{(1+i\Delta_1)\pi}\int_0^\pi\frac{1+\cos\theta}{\Pi(0)}d\theta+F(t)\,, \tag{35}$$

where

$$\Pi(0)=1+\frac{I\,|u_1(r)|^2}{1+\Delta_1^2}\rightarrow 1+\frac{I}{1+\Delta_1^2}(1+\cos\theta)\,,$$

and the correlations of the noise terms $F(t)$ are given by Eq. (14) with $\delta=0$ but replacing

$$\Lambda\rightarrow\frac{1}{\pi}\int_0^\pi(1+\cos\theta)\bar{\Lambda}\,d\theta\,,$$

$$R\rightarrow\frac{1}{\pi}\int_0^\pi(1+\cos\theta)\bar{R}\,d\theta\,,$$

$\bar{R}$ and $\bar{\Lambda}$ have the functional forms of R and Λ of (15) but replacing I with $I(1+\cos\theta)$. We now need to distinguish between the pump and sideband cavities and hence the notation κ_1 and $C_1=g^2N/\gamma_\perp\kappa_1$ to describe the pump cavity relaxation rate and cooperativity parameter, respectively. The integral may be evaluated for the deterministic part of the equation to give a standing-wave deterministic equation

$$\dot{\alpha}_1=E-\kappa_1(1+i\phi_1)\alpha_1$$

$$-\frac{2C_1\kappa_1\alpha_1}{I}(1-i\Delta_1)\left[1-1\Big/\left[1+\frac{2I}{1+\Delta_1^2}\right]^{1/2}\right]. \tag{36}$$

The noise term averages for $\delta=0$ have been presented by Reid and Walls.[24]

Similarly equations for the sideband modes may be written

$$\begin{aligned}\dot{\alpha}_2&=-\kappa(1+i\phi)\alpha_2\\&\quad+\kappa\alpha_2\int_V|u_2(r)|^2[\bar{\gamma}_R(\delta)+i\bar{\gamma}_I(\delta)]d^3r\\&\quad+\kappa e^{2i\theta_0}\alpha_3^\dagger\int_V u_3^*(r)u_2^*(r)\bar{\chi}(\delta)d^3r+F_2(t)\,,\\\dot{\alpha}_3&=-\kappa(1+i\phi)\alpha_3\\&\quad+\kappa\alpha_3\int_V|u_3(r)|^2[\bar{\gamma}_R(-\delta)+i\bar{\gamma}_I(-\delta)]d^3r\\&\quad+\kappa e^{2i\theta_0}\alpha_2^\dagger\int_V u_3^*(r)u_2^*(r)\bar{\chi}(-\delta)d^3r+F_3(t)\,.\end{aligned} \tag{37}$$

The nonzero noise correlations are written [compare Eq. (14)]

$$\langle F_2(t)F_3(t')\rangle=\kappa\,\mathrm{Re}^{2i\theta_0}\delta(t-t')\,,$$

$$\langle F_m^\dagger(t)F_m(t')\rangle=\kappa\Lambda_m\delta(t-t')\quad(m=1,2)\,,$$

where

$$\Lambda_m=\int_V|u_m(r)|^2\bar{\Lambda}\,d^3r\,,$$

$$R=\int_V|u_2^*(r)u_3^*(r)|\,\bar{R}\,d^3r\,.$$

The quantities $\bar{\gamma}_R(\delta),\ldots,\bar{\Lambda},\bar{R}$ have the same functional form as $\gamma_R(\delta),\ldots,\Lambda,R$ defined in Eqs. (15) but with $\alpha_1\rightarrow\alpha_1u_1(r)$, i.e., $I\rightarrow I(1+\cos\theta)$. With the assumption that $\mathbf{k}_2\sim\mathbf{k}_3\sim\mathbf{k}_1$, these integrals may be simplified to the form

$$\begin{aligned}\dot{\alpha}_2&=-\kappa[1+i\phi+\tilde{\gamma}_R(\delta)+i\tilde{\gamma}_I(\delta)]+\kappa\tilde{\chi}(\delta)\alpha_3^\dagger+F_2(t)\,,\\\dot{\alpha}_3&=-\kappa[1+i\phi+\tilde{\gamma}_R(-\delta)+i\tilde{\gamma}_I(-\delta)]\\&\quad+\kappa\tilde{\chi}(-\delta)\alpha_2^\dagger+F_3(t)\,,\end{aligned} \tag{38}$$

where, for example,

$$\tilde{\gamma}_R(\delta)=\frac{1}{\pi}\int_0^\pi(1+\cos\theta)\bar{\gamma}_R(\delta)d\theta\,,$$

and similarly for $\tilde{\gamma}_i(\delta),\ldots$. Although an analytical expression for these averages is possible, it was found more convenient to evaluate the integrals numerically.

A comparison of standing-wave versus ring cavity results for squeezing is illustrated in Fig. 16. Essentially, the nonlinearity increases more significantly at lower intensities for a standing-wave cavity, and, hence the better squeezing at lower intensities. We notice from the degenerate $\delta=0$ situation that the desqueezing effect of fluorescence as one increases the pump intensity is more significant in the standing-wave cavity. This is exemplified in conditions derived by Reid and Walls to avoid spontaneous emission in the degenerate situation: $10I^2/\Delta_1^3\ll 1$ for the standing-wave cavity[24] as compared to $I^2/\Delta_1^3\ll 1$ for a ring cavity.[27]

The theory has assumed a high-Q cavity in a stricter sense than that needed to neglect spatial fluctuations. The

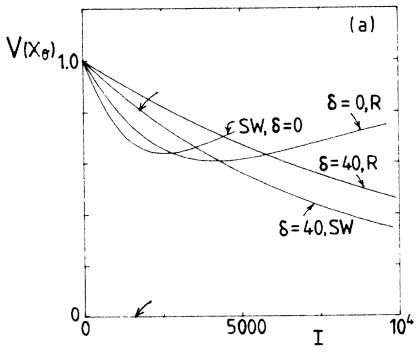

FIG. 16. Squeezing $V(X_\theta,\delta)$ comparison for a ring cavity (R) and a standing-wave cavity (SW): $\Delta_1=-300$, $C=750$. $\delta=40$ is believed to correspond to the experiment (Ref. 12). Region marked by arrows corresponds to $I/I_s=0.02$, where $I_s=\Delta_1^2$ is the saturation intensity. We have selected $\phi=-\gamma_I(\delta)$ so that approximate resonance is obtained between the external laser and the nonlinear pump cavity.

atomic variables have been adiabatically eliminated under the high-Q cavity assumption $\kappa \ll \gamma_\perp$. Figure 17 plots the best squeezing possible, for the optimal phase quadrature θ, in the output field at the sidebands for a perfectly high-Q cavity. The spectrum of squeezing about the sideband frequency in such a high-Q cavity ($\kappa \ll \gamma_\perp$) is essentially a negative Lorentzian (width κ) and the best squeezing is usually obtained at the center (sideband) frequency. We stress that this may not be the case in the experiment where $\kappa \sim \gamma_\perp$ and the high-Q cavity (adiabatic elimination of atomic variables) assumption does not hold. The best squeezing in this case $\kappa \sim \gamma_\perp$ for the resonant mode $\delta=0$ is not necessarily at the center frequency.[51] An analysis of the spectrum of squeezing at the sideband frequencies without making the adiabatic elimination assumption is thus required and is presently in progress.

However, the results presented in Fig. 17 for the output sideband frequency from a high-Q cavity can still give us an insight into the spontaneous emission limits to squeezing for the experiment. This is particularly in view of the fact that recent work[51] on comparison of high- Q and low-Q cavities reveal results for the squeezing at the center of the spectrum (i.e., precisely at the frequency $\omega_L+\epsilon$) to be insensitive to the adiabatic elimination approximation.

The plot Fig. 17 is the squeezing versus the intracavity pump intensity (in units of the saturation intensity $I_s \sim \Delta_1^2$), for the following values currently believed to correspond to the Slusher experiment: $\Delta_1=-300$, $C=750$, $\delta=40$. The several values of cavity detuning ϕ [(ii) and (iii)] discussed in the preceding Sec. V are plotted. The curve $\phi=\phi_R=-\gamma_I(\delta)$ is for the pump laser readjusted in frequency at each intensity so that it is approximately resonant with the dressed pump cavity *at all intensities.* It thus accounts for the nonlinear refractive index term $\gamma_I(\delta)$. This is believed to best correspond to the experiment. Being on resonance with the cavity, this value of cavity detuning allows good squeezing at the lowest possible intensity I, and good squeezing is maintained at higher intensities. Also plotted is the squeezing curve for a fixed cavity detuning $\phi \sim 2C/\Delta_1$, corresponding to adjustment of the pump frequency to take into account the linear refractive index $2C/\Delta_1$ of the medium. The squeezing is reduced at higher intensities for this situation as the detuning between cavity and pump increases. The range of intensity giving good squeezing is narrower at the choice $\phi \sim 2C/\Delta_1$. Also plotted is the squeezing for a cavity detuning $\phi=0$. The squeezing is reduced (compared to the case $\phi \sim 2C/\Delta_1$) at low intensities, because of the detuning between cavity and driving field. However, at higher intensities saturating the atoms, the dispersive response $\gamma_I(\delta)$ decreases and the cavity moves back into resonance with the driving field. Thus the squeezing improves for this case $\phi=0$ at higher intensities. These effects have been well discussed in the preceding Sec. V.

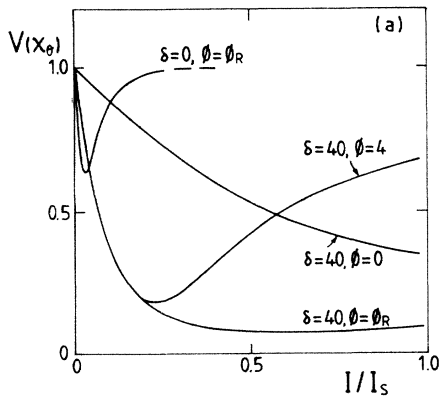

FIG. 17. Squeezing $V(X_\theta,\delta)$ for parameters $\Delta_1=-300$, $C=750$. $\delta=40$ is believed to correspond to the experiment (Ref. 12). Versus intensity I in units of the saturation intensity $I_s=\Delta_1^2=9\times10^4$. Various values of ϕ are selected. $\phi_R=-\gamma_I(\delta)$.

The key feature to be noted from the result Fig. 17, concerns the spontaneous emission limit to squeezing for the nondegenerate $\delta=40$ situation. We have calculated as a comparison the squeezing predicted for *degenerate* $\delta=0$ four-wave mixing. We see that the best squeezing then occurs at lower intensities I and is reduced compared to the nondegenerate situation. This is because of the increase in the fluorescence at $\delta=0$ as one increases the pump intensity. This is not the case for the nondegenerate situation $\delta=40$ corresponding to the experiment, because we are several atomic linewidths detuned from the central pump frequency. Thus, considerably more squeezing is attainable in principle in the nondegenerate scheme by further increasing the pump intensity and thus the nonlinearity of the cavity.

The present Slusher *et al.* experiment is operating in a regime of very low intensity ($I/I_s \sim 0.02$) (Fig. 16). We notice that there is less difference between degenerate and nondegenerate predictions in regimes of low intensity than in the higher intensity regimes. In fact, a theory based on the degenerate $\delta=0$ noise terms derived by Reid and Walls[24] has been presented by Klauder *et al.*[54] for the experiment, and includes additional effects such as phase jitter. It shows quite reasonable agreement with the present experiment. A theory based on degenerate $\delta=0$ noise terms, however, would wrongly indicate that fluorescence kills the squeezing at even moderate intensities. We also note that in this present experimental regime of very low nonlinearity, the degenerate situation $\delta=0$ gives better squeezing than the nondegenerate $\delta=40$, for the particular value of intensity $I/I_s \sim 0.02$ [see Fig. 11(b), $I=300$].

We make a final comment concerning the role of the pump in determining the squeezing generated from the squeezing cavity. From Eqs. (37), we see that the relevant pump parameters are the intensity I at the medium, and the detuning ϕ between the pump laser of frequency ω_L and the central resonant mode ω_1 of the squeezing cavity. It is the frequency of the laser ω_L which is relevant since this determines the frequency for the medium polarization v_I [Eq. (7)]. The results given above for the squeezing generated from the squeezing cavity thus may also apply to the situation where one has no pump cavity but simply a pump laser of frequency ω_L pumping the medium.

VII. CONCLUSION

We have presented a quantum theory of nondegenerate four-wave mixing via N two-level atoms in a single-port

cavity. The pump cavity is driven by an external driving field detuned from the cavity by ϕ (in units of the cavity relaxation rate κ) and forms a steady-state intracavity pump intensity I (in units of the resonant saturation intensity for the medium). The external pump field is detuned Δ_1 atomic linewidths from the atomic resonance. We assume pure radiative damping. The four-wave mixing occurs between the pump mode and two sideband modes separated in frequency from the pump by $\pm\delta$, in units of the longitudinal relaxation rate for the two-level atom.

We have calculated the squeezing in the steady-state transmitted field external to the cavity at the sidebands under the assumption of a high-Q cavity where the atoms relax much more quickly than the field ($\gamma_\perp$, $\gamma_\parallel \gg \kappa$) and the variables may be adiabatically eliminated. The solution is valid for regimes where the zero deterministic steady-state solution for the sidemode amplitudes is stable. Although the deterministic steady-state solution is zero, intensity builds up in the sidemodes because of spontaneous emission. Our theory assumes small intensity fluctuations and is linear in the sidemode amplitudes, not taking into account any feedback effects of the sideband intensity on the pump.

Our aim has been to study possibilities for optimizing squeezing via nondegenerate four-wave mixing. The two-level atom provides the nonlinear coupling $\chi(\delta)$ between the three modes and that which squeezes the light. The squeezing becomes significant as the nonlinearity of the cavity increases [$|\chi(\delta)| \sim 1$] so that threshold is approached. However, the medium also absorbs radiation $\gamma_R(\delta)$ and induces a phase-insensitive fluorescence radiation Λ. The absorption $\gamma_R(\delta)$ and fluorescence Λ are phase insensitive thus tending in general to destroy the squeezing generated via the phase-sensitive coupling process $\chi(\delta)$. In addition, there is the dispersive response of the medium $\gamma_I(\delta)$ which introduces a change in the resonant frequency of the nonlinear dressed cavity. Significant detuning between the external pump field and the nonlinear dressed cavity will tend to decrease the effective nonlinearity and hence the squeezing. We require, for example, greater $|\chi(\delta)|$ to obtain threshold [for example, the threshold condition at $\delta=0$ becomes $|\chi(0)| = |\gamma(0)|$].

The spectra $\chi(\delta), \Lambda, \gamma_R(\delta), \gamma_I(\delta), \ldots$, have been calculated and discussed in some detail. There are four distinctive regimes: $\delta=0$ corresponding to degenerate four-wave mixing; a sideband detuning of several atomic linewidths but less than the Rabi frequency $\frac{1}{2}(2I+\Delta_1^2)^{1/2}$; the regime δ at the Rabi frequency; and δ well beyond the Rabi frequency. We have considered in some detail the case of $\Delta_1=100$, a well-detuned atom, and revise the major features of the various spectra.

The coupling spectrum $\chi(\delta)$ [Fig. 6(c)] shows broad peaks at the Rabi frequencies $\delta=\pm\frac{1}{2}(2I+\Delta_1^2)^{1/2}$ and relatively flat regimes of significant coupling $\{\chi(0) \sim 2CI/\Delta_1(1+\Delta_1^2)[1+I/(1+\Delta_1^2)]^2\}$ between the Rabi frequencies. The enhancement of the coupling at the Rabi frequencies is particularly significant at higher intensities and is understood by the coupling process depicted in Fig. 3. Beyond the Rabi frequencies the coupling decreases. The magnitude of the coupling is small at low intensities but increases with increasing intensity, reaching a maximum at the saturation intensity $I \sim \Delta_1^2$, and then decreasing as the medium continues to saturate. The absorption $\gamma_R(\delta)$ and dispersion $\gamma_I(\delta)$ have nonzero linear components and are thus significant at low intensities I, e.g., $\gamma_R(0)=2C/(1+\Delta_1^2)[1+I/(1+\Delta_1^2)]^2$ and $\gamma_I(0) = -2C\Delta_1/(1+\Delta_1^2)[1+I(1+\Delta_1^2)]^2$. At low intensities the absorption [Fig. 4(c)] shows a large absorption peak at the Rabi frequency coinciding with the atomic resonance. This absorption tends to destroy squeezing. The absorption, however, saturates more readily than the coupling and becomes insignificant (provided one is away from the narrow resonances at the Rabi frequencies) at intensities above the saturation intensity $I_s \sim \Delta_1^2$. We notice at such high intensities that the absorption profile shows absorption at the Rabi frequency closest to the atomic resonance ω_0 but gain at the other Rabi frequency. This gain results also from the resonant process depicted in Fig. 3(b) coupling sidebands detuned at the Rabi frequencies $\pm\frac{1}{2}(2I+\Delta_1^2)^{1/2}$. The resonant coupling process generates good squeezing at the Rabi frequencies for intensities saturating the atoms.

At such higher intensities the fluorescence Λ increases (Fig. 7). It is at these higher intensities saturating the atoms that nondegenerate four-wave mixing is clearly advantageous. The fluorescence spectrum then has three peaks positioned at $\delta=0\pm\frac{1}{2}(2I+\Delta_1^2)^{1/2}$. There is a significant central peak at $\delta=0$. This is in contrast to the coupling spectrum which has no significant central peak. Because of the central fluorescence peak, degenerate four-wave mixing $\delta=0$ is not so suitable for generation of squeezed light.

The fluorescence spectrum Λ, however, reduces significantly between peaks, as compared to the coupling. Thus, by increasing the sideband detuning over several orders of atomic linewidth ($\delta \gtrsim 2$), dominance of the coupling becomes possible. Good squeezing is then possible provided the coupling is sufficient in absolute terms and that the absolute absorption and detuning of the external driving field from the nonlinear cavity is insignificant (Fig. 11). At sufficiently high intensities $I > \Delta_1^2$ well above saturation the absorption and dispersive terms are indeed small. One obtains approximate resonance of the driving field with the nonlinear cavity for all intensities by setting the cavity detuning $\phi=-\gamma_I(0)$. For the high intensities we are considering, however, $\gamma_I(\delta)$ becomes very small as the medium saturates and one can obtain good squeezing for $\phi \to 0$ [Fig. 13(b)].

As the sideband detuning increases to approach the Rabi frequency [$\delta \to \frac{1}{2}(2I+\Delta_1^2)^{1/2}$], the broad coupling peak is encountered first and coupling increases, thus increasing the squeezing. The behavior of the two-level atom in this regime of $0 \ll \delta < \frac{1}{2}(2I+\Delta_1^2)^{1/2}$, such that absorption $\gamma_R(\delta)$ is small but coupling $\chi(\delta)$ significant, is like that of the dispersive ideal squeezer (22). Increasing δ further to coincide with the Rabi frequency $\delta = \frac{1}{2}(2I+\Delta_1^2)^{1/2}$, one encounters the narrow (width $\sim\gamma_\perp$) resonant peaks of the spectra $\gamma_R(\delta)$, $\chi_R(\delta)$, Λ, etc. The behavior of the atomic medium is no longer that of a dispersive medium. Good squeezing is possible however

[Figs. 13(f) and 14] because of the resonant process depicted in Fig. 3(b). This is not true at lower intensities below saturation [Fig. 3(a)] where loss is still important and increases significantly at the Rabi frequency destroying the squeezing (Fig. 11). In many cases, however, the increase in coupling near the Rabi frequency results in instability where our theory no longer holds. Well beyond the Rabi frequency the nonlinear coupling and thus the squeezing diminishes.

Good squeezing is possible for a broad range of cavity cooperativity C values provided one increases the intensity sufficiently. Lower C values ($2C \ll \Delta_1^2$) require high intensities to attain sufficient nonlinearity, but this is no difficulty providing one can increase the sidemode detuning δ to avoid the central fluorescence peak [Fig. 11(a)]. Lowering the C value too much, however, will reduce the nonlinearity and hence the squeezing obtainable before saturation sets in. For higher C values ($2C > \Delta_1^2$) it is possible to attain significant nonlinearity with lower intensities (below saturation). The absorption γ_R, however, is increased and tends to reduce the squeezing possible [Fig. 13(e)]. However, the absorption profile saturates more readily than the coupling. Thus it is possible to obtain good squeezing by increasing the intensity sufficiently (well above saturation) to saturate the absorption, while still maintaining sufficient nonlinearity [Fig. 13(f)].

We have studied in this paper the effect of enhanced coupling between sideband modes detuned from the central pump mode by frequencies approaching the Rabi frequencies in a two-level atomic medium. We have shown how phase-insensitive atomic fluorescence is minimized provided one can look for squeezing in a sideband mode detuned several atomic linewidths from the central pump mode. In a limiting high-Q cavity ($\kappa \ll \gamma_\perp, \gamma_\parallel$) such as considered here, the width of the transmitted spectrum of the external central pump ($\delta = 0$) is determined by the cavity linewidth κ and is thus always within the central fluorescence peak. Hence we are required to look at adjacent cavity modes. In a low-Q cavity ($\kappa \gg \gamma_\perp, \gamma_\parallel$), however, the transmitted spectrum of the central pump mode broadens until determined by the atomic linewidth $\gamma_\perp$. Thus the effects described in this paper can also be observed in the transmitted field of a single mode low-Q cavity. The results for this case are discussed in Ref. 51. The limiting "low-Q" ($\gamma_\perp \ll \kappa$) cavity has identical output squeezing spectra to those presented here.

Our work indicates that by saturating the atoms in a nondegenerate four-wave mixing scheme one can avoid spontaneous emission due to the atoms and yet maintain sufficient four-wave-mixing coupling to produce good squeezing in the transmitted light. This is possible for a broad range of cavity cooperativity C values and sidemode detunings δ. Good squeezing is possible at low atomic detunings ($\Delta_1 \sim 4$) for δ corresponding to the Rabi frequencies and at intensities sufficient to saturate the atoms. Although squeezing is best achieved in general by keeping the external pump approximately resonant with the nonlinear pump cavity [$\phi = -\gamma_I(0)$], good squeezing is still possible in the vicinity of the Rabi sidepeaks for fixed ϕ not quite resonant, in particular for $\phi = 0$ at high intensities. It would seem that good squeezing is possible for a wide range of cavity situations.

ACKNOWLEDGMENT

The authors are grateful for financial support from the New Zealand University Grants Committee, and would like to acknowledge work partially supported by the U.S. Office of Naval Research.

[1]D. Stoler, Phys. Rev. D **1**, 3217 (1970).
[2]H. P. Yuen, Phys. Rev. A **13**, 2226 (1976).
[3]C. M. Caves, Phys. Rev. D **230**, 1693 (1981).
[4]H. P. Yuen and J. H. Shapiro, IEEE Trans. Inf. Theory **24**, 657 (1978); **26**, 78 (1980).
[5]D. F. Walls, Nature **306**, 141 (1983).
[6]R. S. Bondurant, P. Kumar, J. H. Shapiro, and M. Maeda, Phys. Rev. A **30**, 343 (1984).
[7]M. D. Levenson, R. M. Shelby, A. Aspect, M. D. Reid, and D. F. Walls, Phys. Rev. A **32**, 1550 (1985).
[8]M. D. Levenson, R. M. Shelby, and S. H. Perlmutter, Opt. Lett. **10**, 514 (1985).
[9]R. M. Shelby, M. D. Levenson, D. F. Walls, G. J. Milburn, A. Aspect, Phys. Rev. A **33**, 4008 (1986).
[10]M. D. Levenson and R. M. Shelby, in *Quantum Optics IV*, edited by J. D. Harvey and D. F. Walls (Springer, New York, 1986).
[11]R. E. Slusher, L. W. Hollberg, B. Yurke, J. C. Mertz, and J. F. Valley, Phys. Rev. A **31**, 3512 (1985).
[12]R. E. Slusher, L. W. Hollberg, B. Yurke, J. C. Mertz, and J. F. Valley, Phys. Rev. Lett. **55**, 2409 (1985).
[13]R. E. Slusher and B. Yurke, in *Frontiers in Quantum Optics*, edited by S. Sartar and E. R. Pike (Hilger, London, 1986).
[14]R. E. Slusher and B. Yurke, in *Quantum Optics IV*, edited by J. D. Harvey and D. F. Walls (Springer, New York, 1986).
[15]H. J. Kimble and J. Hall, in *Quantum Optics IV*, edited by J. D. Harvey and D. F. Walls (Springer, New York, 1986).
[16]G. J. Milburn and D. F. Walls, Opt. Commun. **39**, 410 (1981).
[17]L. A. Lugiato and G. Strini, Opt. Commun. **41**, 67 (1982).
[18]B. Yurke, Phys. Rev. A **29**, 408 (1984).
[19]M. J. Collett and C. W. Gardiner, Phys. Rev. A **30**, 1386 (1984).
[20]C. W. Gardiner and C. M. Savage, Opt. Commun. **50**, 173 (1984).
[21]H. P. Yuen and J. H. Shapiro, Opt. Lett. **4**, 334 (1979).
[22]P. Kumar and J. H. Shapiro, Phys. Rev. A **30**, 1568 (1984).
[23]M. D. Reid and D. F. Walls, Opt. Commun. **50**, 406 (1984).
[24]M. D. Reid and D. F. Walls, Phys. Rev. A **31**, 1622 (1985).
[25]B. Yurke, Phys. Rev. A **32**, 300 (1985).
[26]M. J. Collett and D. F. Walls, Phys. Rev. A **32**, 2887 (1985).
[27]M. D. Reid and D. F. Walls, Phys. Rev. A **32**, 396 (1985).
[28]L. A. Lugiato and G. Strini, Opt. Commun. **41**, 447 (1982).
[29]M. D. Reid and D. F. Walls, Phys. Rev. A **28**, 332 (1983).
[30]C. Savage and D. F. Walls, Phys. Rev. A **33**, 3282 (1986).

[31]L. A. Lugiato, G. Strini, and F. de Martini, Opt. Lett. **8**, 256 (1983).
[32]D. F. Walls and P. Zoller, Phys. Rev. Lett. **47**, 709 (1981).
[33]M. J. Collett, D. F. Walls, and P. Zoller, Opt. Commun. **52**, 145 (1984).
[34]H. J. Carmichael, Phys. Rev. Lett. **55**, 2790 (1985).
[35]A. Heidmann, J. M. Raimond, and S. Reynaud, Phys. Rev. Lett. **54**, 326 (1985).
[36]M. Butler and P. D. Drummond, Opt. Acta 33, 1 (1986).
[37]B. J. Dalton, in *Quantum Optics IV,* edited by J. D. Harvey and D. F. Walls (Springer-Verlag, Berlin, 1986).
[38]H. Haken, *Handbuch der Physik* (Springer-Verlag, Berlin, 1970), Vol. XXV/2C.
[39]P. D. Drummond and D. F. Walls, Phys. Rev. A **23**, 2563 (1981).
[40]M. D. Reid and D. F. Walls, JOSA B **2**, 1682 (1985).
[41]M. D. Reid, D. F. Walls, and B. J. Dalton, Phys. Rev. Lett. **55**, 1288 (1985).
[42]P. Anantha Lakshmi and G. S. Agarwal, Phys. Rev. A **32**, 1643 (1985).
[43]T. Fu and M. Sargent, Opt. Lett. **4**, 366 (1979).
[44]R. W. Boyd, M. G. Raymer, P. Narum, and D. J. Marten, Phys. Rev. A **24**, 411 (1981).
[45]M. Sargent III, M. O. Scully, and W. E. Lamb, Jr., *Laser Physics* (Addison-Wesley, Reading, Mass., 1974).
[46]M. Sargent III, M. Zubairy, and F. de Martini, Opt. Lett. **8**, 76 (1983).
[47]M. Sargent III, D. A. Holm, and M. Zubairy, Phys. Rev. A **31**, 3112 (1985).
[48]S. Stenholm, D. A. Holm, and M. Sargent III, Phys. Rev. A **31**, 3124 (1985).
[49]M. D. Reid and D. F. Walls, Phys. Rev. A **33**, 4465 (1986).
[50]D. F. Walls and M. D. Reid, in *Frontiers of Quantum Optics,* edited by S. Sarkar and E. R. Pike (Hilger, London, 1986).
[51]M. D. Reid, A. Lane, and D. F. Walls, in *Quantum Optics IV,* edited by J. D. Harvey and D. F. Walls (Springer, New York, 1986).
[52]D. Holm and M. Sargent, Phys. Rev. A **33**, 4001 (1986).
[53]C. W. Gardiner and M. J. Collett, Phys. Rev. A **31**, 3761 (1985).
[54]J. R. Klauder, S. McCall, and B. Yurke, Phys. Rev. A **33**, 3204 (1986).
[55]W. H. Liousell, *Quantum Statistical Properties of Radiation* (Wiley, New York, 1973).
[56]P. D. Drummond and C. W. Gardiner, J. Phys. **13A**, 2353 (1980).
[57]D. Holm, M. Sargent III, and B. Capron, Opt. Lett., **11**, 443 (1986).
[58]D. Holm (private communication).
[59]B. L. Schumaker and C. M. Caves, in *Coherence and Quantum Optics V,* edited by Mandel and Wolf (Plenum, New York, 1984).
[60]C. M. Caves and B. L. Schumaker, Phys. Rev. A **31**, 3068 (1985); B. L. Schumaker and C. M. Caves, *ibid.* **31**, 3093 (1985).
[61]R. Bonafacio and L. A. Lugiato, Lett. Nuovo Cimento **21**, 517 (1978).
[62]S. S. Hassan, P. D. Drummond, and D. F. Walls, Opt. Commun. **27**, 480 (1978).
[63]C. W. Gardiner, *Handbook of Stochastic Methods in Physics, Chemistry and Natural Sciences* (Springer-Verlag, Berlin, 1983).
[64]P. D. Drummond and D. F. Walls, J. Phys. A **13**, 725 (1980).
[65]L. A. Lugiato, Nuovo Cimento B **50**, 89 (1979).
[66]H. J. Carmichael, D. F. Walls, P. D. Drummond, and S. S. Hassan, Phys. Rev. A **27**, 3112 (1983).